Revision of Manuscript: "Soil dielectric characterization during freeze-thaw transitions using L-band coaxial probe and soil moisture probes" by Alex Mavrovic *et al.*

In blue: Reviewer's comments.
R= Reviewer; P = Page; L = Line as they appear in the Original manuscript version
G= General comment followed by numbering

In black: Answers to referees.
P=Page; L=Line; Track change version
In black and italic: Modification added to text.

Comments from the Reviewers:

Reviewer #1:

Synopsis:

This manuscript describes a laboratory experiment in which the relative dielectric permittivity at L-band of a variety of different types of soil are measured during the freeze <-> thaw process with a dedicated microwave open-ended coaxial probe (OECP) and a commercial soil moisture probe: Hydraprobe (HP). The measurements with both the OECP and HP show a clear hysteresis effect associated with the freeze and thaw process in the graphs of complex relative dielectric permittivity (epsilon) versus soil temperature. Although there are some differences in the measured epsilon between the OECP and HP the authors argue that soil moisture sensors such as HP, which are relatively cheap, tested and verified, can be used construct validation networks for passive microwave remote sensing. Additionally, the manuscript addresses that current models for soil epsilon don't incorporate the freeze <-> thaw hysteresis effect.

The experiment, its results, and proposed application in building validation networks for soil dielectric permittivity with soil moisture probes, I consider as a valuable contribution to the microwave remote sensing community. The title does not fully reflect the contents of the paper, I think you could add "with a soil moisture probe" in the end. Description of the experimental design should be improved. Also the description and explanation of the observed freeze <-> thaw hysteresis should be more elaborate. Finally, throughout the paper the structure of the sentences can be improved.

We made substantial improvement to the manuscript by adding more details on the experimental design and the models' equations and assumptions. The explanations of the freeze/thaw hysteresis effect were also expended to highlight the impact of the temperature transition speed and the temperature sensing volume versus the permittivity sensing volume on the hysteresis amplitude. Finally, the title was adjusted to better reflect the objectives of the study.

Specific comments:

[1] R1, P6, L188 and Fig. 3: "The OECP and HP were fully… " Why was the OECP inside the OBS soil sample and not inside the other three soil samples? And if it was buried inside the OBS sample would not this disturb the sample? I suppose the sample structure was better preserved in the configuration of figure 3b.

The OECP was buried in the OBS soil sample by digging a small-scale trench, alike soil moisture probes are generally installed in the field. The horizontal position of the OECP fully places the probed volume in the undisturbed soil. The OECP was fully buried in the OBS soil sample to simplify the installation. Since the other three samples were smaller, the setup requires that part of the OECP stands out of the container to assure the probed volume stays within the soil samples. Details were added to this paragraph about the experimental setup.

P6-7, L212-214: The OECP and HP were *horizontally inserted into undisturbed soil* and centered at a depth of 2.5 cm below the soil surface *with sufficient spacing between the probes and the soil samples edges to ensure that the probed volumes are restricted to the limits of the soil samples* (Fig. 3).

[2] R1, G1: General remark on the samples and measurement setup. With the OBS sample HP measurements were taken at three positions. As Figure 5 shows the measured responses at these three positions varies. Why were there not also measurements at multiple positions for the OECP with the OBS sample? And why were the other 3 samples not also measured with the HP (and the OECP) at multiple positions? Was this because the OBS sample was expected to be less homogeneous due to the organic content? And why only one sample per soil type was measured? The choices the authors made in this regard should be explained in the text, even if simply for practical reasons.

The OECP is a promising instrument currently developed by the Université de Trois-Rivières and Université de Sherbrooke. Only one OECP was available for the experiment. Logistics is the primary reason for the difference in setup between the OBS soil samples and the others, the soil sample collections were not made in the same type of container for all sites. Even if the cylinder samples are smaller in size, the probed were properly positioned to ensure reliable measurements (see previous response to comment R1[1]). The repeatability of the measurements gives us confidence that the experimental protocol is robust. The explanation for the two distinct setups was added.

P7, L216-218: *The Fig. 3a and 3b setup discrepancies only reflect the two distinct containers used for soil collection at different sites, both configurations ensured sufficient spacing for undisturbed measurements.*

[3] R1, P7, L243: The amplification of the hysteresis -effect by the setup, is it possible to explain this in the text with a few sentences? You refer to this hysteresis amplification later on, it would be better if the reader could find an explanation for this effect in this manuscript rather than somewhere else (the reference). You can of course leave the reference.

Further explanations and reference were added.

P8-9, L286-291: Hysteresis effects can be observed between the freezing and thawing cycles in Figs. 5 through 8*, i.e. a different behavior of permittivity variation depending on whether the ground freezes or thaws*. Although hysteresis *is reported in soil freezing studies, this effect was amplified by the temperature transition speed and differences in the sensing volume for temperature and permittivity observations (Pardo Lara et al., 2020)*. Fig. 11 shows a slow freeze/thaw transition displaying a hysteresis effect of diminished amplitude, but still noticeable.

P9-10, L321-323: Even if amplified by the experimental setup, the hysteresis effect between the freezing and thawing cycles is not simulated by any model since *they do not include the evolution of soil properties in time*.

[4] R1, P8, L252-255: I am not sure whether I completely agree with your explanation. You ascribe the difference in measured transition to the different probing volumes of both sensors and that with the HP there is a longer time required for the freezing/thawing front to penetrate the probed volume. The way I see it for both sensors the temperature gradient is from top/bottom (because of your nice trick of placing sand around the sample) so ideally the progression of this freezing/thawing front is the same for both sensors. What is different is the diameter of the sensor's probing volume, see Figure 2. For the OECP this is roughly half the diameter of the HP, which would explain a more abrupt transition. Another difference is the length of the probing volume. For wet conditions the length for the HP is about 15x that of the OECP. The way I see it the HP then performs 15 OECP measurements at 15 different positions. If there is variation in the soil over this length, the HP then shows a kind of average transition over all these 15 volumes. This is the reason I was also wondering why the OECP was not used at multiple positions within one sample (comment [2]). You could maybe test your volume explanation by taking the OECP result and scale it to the HP volume.

We agree that the freezing/thawing front is mostly vertically oriented and therefore is the probes' volume diameter difference that is mostly responsible for the difference in transition steepness. Clarifications about the point were added. The suggested experiment of using several OECP at different positions is a relevant one, but as mentioned previously, only one probe was available for the experiment, while removing the probe to measure at different depths would have changed the soil properties. Comparing the average of several OECP measurements to the HP measurement would possibly give further insights on the OECP and HP comparability.

P9, L311-315: Since the instruments measure an average permittivity for the whole probed volume, *the* larger probed volume *of the HP* record an extended freeze/thaw transition because of the longer time required for the freezing/thawing fronts to penetrate the depth of volume probed. *Since the freezing/thawing front is mostly vertically oriented, it is the difference in probes' sensing diameter that causes the difference in transition steepness.*

[5] R1, Fig. 5-8: During the thawing process there appears to be maximum epsilon' and epsilon" directly after the main thawing process after which the epsilon' and epsilon" decrease again slightly. This is effect is most pronounced in Figure 7. Do you have an explanation for this effect?

It is suspected that this effect is due to water percolation during thawing, but further investigation is needed to confirm this phenomenon. This hypothesis was added to the discussion.

P9, L306-309: *In most experiments presented, a short surge in permittivity can be observed right after thawing, followed by a small drop leading to a convergence to a relatively stable permittivity value associated with a fully thawed soil. Further investigation is needed to see if this short surge could be related to moisture migration toward the thawing front and to water percolation through the soil sample toward the end of the thawing transition.*

[6] R1, P8, L270-272: Based on the Figures 5 - 8 I find the freeze/thaw transitions not similar. Can the differences of the OECP and HP measurements be explained by the difference in probing volume? Also you mention that the main difference between the OECP and HP measurements are the epsilon values at the end of the cycle, at the "stable plateaus" as you call it. But isn't the hysteresis just as important? Perhaps if a found calibration equation for a given soil is applied to the HP results the freeze/thaw hysteresis is more like that of the OECP?

It is correct that the difference in freeze/thaw transition steepness could be explained by the difference in probing volume. The authors share the same point of view that this is probably the main explanation and it is put forward in the Experimental Results section (4.1).

The fully frozen/thawed values comparison between measurements and models consist of the strongest differences observed in this study. The hysteresis is of equal importance, but the trends are similar between the permittivity measurements. This is to say that the hysteresis effect occurs at very similar temperatures.

It is typical to use soil specific calibration equation to produce soil moisture estimates from HP raw permittivity measurements. However, the HP instrument does not allow for customized calibration equation to compute permittivity from raw reflection coefficients.

P9, L 310-315: It can also be observed that the freeze/thaw transition measurements are *steeper* with the *OECP* than the HP. This is probably due to the HP's larger probed volume. Since the instruments measure an average permittivity for the whole probed volume, a larger probed volume will record a *more extended* freeze/thaw transition because of the longer time required for the freezing/thawing fronts to penetrate the depth of volume probed. *Since the freezing/thawing front is mostly vertically oriented, it is the difference in probes' sensing diameter that causes the difference in transition steepness.*

[7] R1, P8, L283-289: What do the authors want to say with this paragraph? Is the point that, should a network of (tried, tested, and cheap) hydraprobes be installed over a large area as surrogate L-band permittivity sensors (lines 274 – 275), one must realize that the volume over which it measures is not exactly what radiometers probe?

The potential in using already deployed HydraProbes networks is laid out in the previous paragraph. The message of this paragraph is that in the case of freeze/thaw algorithms testing, previous studies have shown that the L-band radiometric signal is sensitive to the freezing of the first centimeter of soil which implies that the OECP would be a more suitable instrument to study that phenomenon due to its inherent smaller sensing volume. The paragraph was reshaped to get this point across more clearly.

P10, L348-351: *Ground- and satellite-based L-band radiometric measurements are very sensitive to the freezing of the first centimeter of soil (Rowlandson et al., 2018; Roy et al., 2017a,b; Williamson et al., 2018). Therefore, the shallower depth (~ 0.4–1 cm) and smaller volume (~4–10 cm^3) probed by the OECP makes it a potentially more suitable instrument to study the freeze/thaw signal observed from L-band radiometers.*

[8] R1, P9, L300: What hypothesis do the authors refer to?

The hypothesis referred is the one proposed in the previous paragraph about the correlation between the hysteresis effect and the temperature transition speed. It was clarified to avoid further confusion.

P11, L362-363: *We further tested the hypothesis that the hysteresis effect is correlated with the temperature transition speed* using an OBS soil sample using a slower freeze/thaw transition rate.

[9] R1, Fig. 11: With the freezing cycle you see both epsilons increase first before they decrease rapidly when all soil freezes. Why don't we see this behaviour during of the freezing fast freeze/thaw experiment? We do see it during the thawing (see comment [5]), are these processes linked?

It is hypothesized that water displacement inside the sample during freezing is responsible for this surge, similar to the explanation of the surge in Fig. 5-8 (see response to comment R1[5]).

[10] R1, P1, L20: You state that you show in the manuscript that the OECP is a suitable device for measuring epsilon… . The demonstration that OECP can measure the epsilon of any homogeneous material is given in your previous studies Mavrovic2018 and Mavrovic2020, not in this manuscript. In this manuscript you use the OECP to quantify the performance of the HP. I propose to change the sentence to .. the OECP measured the frozen soil epsilon' to be 3.5 to 6.0, the epsilon" to be 0.4 – 1.2 etc.

Suggestion applied and text modified.

P1, L21: *The OECP measured the* frozen…

[11] R1, P2, L41-42: Cite not only papers that use the tau-omega model for microwave scattering of vegetation. Give examples of papers that solve the radiative transfer equations differently, such as the Tor Vergata model (Bracaglia, Ferrazzoli, and Guerriero, RSE, 1995) or the MIMICS model (Ulaby, Sarabandi, et al., 1990 IJRS).

References to radiative transfer models added.

P2, L39-42: Information about the physical state of the soil is retrieved from microwave observations by using radiative transfer models to simulate the interaction between electromagnetic waves and the surface (*Attema and Ulaby, 1978; Mo et al., 1982; Ulaby et al., 1990; Bracaglia et al., 1995; Huang et al., 2017*).

P12, L418-419: *Attema, E., and Ulaby, F.: Vegetation modeled as a water cloud. Radio Sci., 13(2), 357-364, doi:10.1029/RS013i002p00357, 1978.*

P13, L429-430: *Bracaglia, M., Ferrazzoli, P., and Guerriero, L.: A fully polarimetric multiple scattering model for crops, Remote Sens. of Environ., 54(3), 170–179, doi:10.1016/0034-4257(95)00151-4, 1995.*

P17, L664-665: *Ulaby, F., Sarabandi, K., McDonald, K., Whitt, M., and Dobson, M.: Michigan microwave canopy scattering model, Int. J. Remote Sens., 11(7), 1223–1253. doi:10.1080/01431169008955090, 1990.*

[12] R1, P2, L50: Propose to change to: "Permittivity is characterized by a complex number, where the real part describes the translation and rotation of molecular dipoles, which drive the wave propagation, and the imaginary part describes the energy loss associated with this process." Further I propose to refer to a textbook on electrodynamics, for example: Griffiths D.J., Introduction to Electrodynamics.

Suggestion implemented. The Griffiths is a well-known reference to the author, it was added.

P2, L52-54: Permittivity is characterized by a complex number, where the real part (ε') describes the *translation and rotation* of molecular dipoles, which drives *the* wave propagation, and the imaginary part (ε'') describes the *energy loss (absorption) associated with this process (Griffiths, 1999)*.

P14, L501-502: *Griffiths, Introduction to electrodynamics - Third Edition, Pearson, Upper Saddle River, New Jersey, 576 pp., 1999.*

[13] R1, P2, L63: remove the word passive here.

``passive`` removed.

P2, L65-66: The permittivity drop observable within freezing soils translates into a higher microwave emission from the ground.

[14] R1, P3, L75: "to collect permittivity estimates", propose to change to "to collect better permittivity estimates." Also "… for the validation of passive microwave instruments". Propose to change to ".. for the validation of microwave radiometric observations". Or something similar, but it's the observations than need to be validated.

Suggestion implemented.

P3, L79-80: Therefore, there is a need to collect *better* permittivity estimates for the validation of *microwave observations and models*.

[15] R1, P3, L86: Add OECP between assess and L-band.

Added.

P3, L91: The goal of this laboratory-based study is to assess *OECP* L-band permittivity measurements…

[16] R1, P4, L109: The reflectometer generates an electromagnetic wave, not only a propagating electric field.

Clarified.

P4, L113-114: This reflectometer acts as both *an electromagnetic wave generator and* a reflection coefficient measuring instrument *for frequencies from 1 to 2 GHz*.

[17] R1, P4, L110: Over what frequency band were the measurements performed?

Specified.

P4, L113-114: This reflectometer acts as both *an electromagnetic wave generator and* a reflection coefficient measuring instrument *for frequencies from 1 to 2 GHz*.

[18] R1, P4, L116: "The penetration depth of the… " This sentence is too vague for my taste. I propose something like: "The sensing depth of the OECP is the maximum depth at which the medium is polarized due to the incident electric field, and as such contributes to the reflection of the EM wave backwards into the coax."

Sentence reworked.

P4, L120-127: The *sensing* depth of the OECP *is* defined as the maximal depth at which a medium is *polarized due to the incident electric field, and as such contributes to the electromagnetic wave reflection*. *The sensing depth is proportional to the medium's permittivity and the magnitude of the electric field generated by the reflectometer*, which

displays a constant power output of 10 dBm (Fig. 1b). The OECP typical *sensing* depth approaches 1 cm under dry soil conditions and the cylindrical probed volume is about 3.5 cm wide in diameter (Figure 2). Under wet soil conditions, the *sensing* depth shrinks down to 0.4 cm.

[19] R1, P4, L118: "The magnitude of this effective electric… " the effective electric field has not been defined or explained previously. I assume you refer the resulting electric field in the medium? Which is the sum of the original electric field coming from the coax E0, which polarizes (rotates and or translates) the molecules and the electric field produced by the rotated or displaced molecules themselves Ed. Latter counters E0, which counters Ed, which counters E0 etc. You end up with a resulting electric field E, which is actually lower in magnitude for a higher epsilon.

The effective electrical field refers here to the extent of the electrical field influencing the reflection coefficient measurements. The use of this term here seems confusing and not necessary. Therefore, it was removed and the sensing depth was directly referenced.

P4, L122-124: *The sensing depth is proportional to the medium's permittivity and the magnitude of the electric field generated by the reflectometer*, which *displays a constant power output of 10 dBm* (Fig. 1b).

[20] R1, P4, L119: You describe the electric field generated by the reflectometer in terms of power (dBm = 1 mW) which is incorrect. I propose to state simply that the generated power is 10 dBm.

Clarified.

P4, L122-124: *The sensing depth is proportional to the medium's permittivity and the magnitude of the electric field generated by the reflectometer*, which *displays a constant power output of 10 dBm* (Fig. 1b).

[21] R1, P4, L131: If applicable, note what type of Hydraprobe you used (for example type A or B100 or …)

Precisions were added on the HydraProbe used for this experiment.

P4, L137: *A digital model of the HP using the SDI-12 protocol was employed.*

[22] R1, P4, L137: ".. it uses the ratio of the incident and reflected waves to numerically solve Maxwell's equations, yielding the impedance and complex permittivity." That the device solves the Maxwell's equations sounds far-fetched to me. One of the papers on found on the Hydraprobe website should provide you with a better (quick) description on how the device works. In my understanding the Hydraprobe indeed works similar to the OECP: The epsilon of the material between the steel tines determines the characteristic impedance (symbol Z0 typically, or its inverse the characteristic admittance Y0) . The reflection of the The steel tines, together with the material (soil) they are in, forms a

microwave transmission line with characteristic impedance Z0 (or its inverse Y0). The reflection coefficient, measured by the device, is dependent on this Z0.

The HydraProbe Soil Sensor User Manual (2018) section 4.4.1 (p.34) on the theory of operation cites more comprehensive references on how the numerical solution of Maxwell's equations is obtained to derive the complex permittivity from impedance measurements. Those references were added.

P4, L141-143: *The HP soil complex permittivity computation is derived from the impedance measurements between the steel tines, which depends mainly on the liquid water content of the soil surrounding the tines (Campbell, 1990; Seyfried and Murdock, 2004).*

P13, L439-440: *Campbell, J.: Dielectric Properties and Influence of Conductivity in Soils at One to Fifty Megahertz, Soil Sci. Soc. Am. J., 54(2), 332-341, doi:10.2136/sssaj1990.03615995005400020006x, 1990.*

P17, L654-655: *Seyfried, M., and Murdock., M.: Measurement of Soil Water Content with a 50-MHz Soil Dielectric Sensor, Soil Sci. Soc. Am. J., 68(2), 394-403, doi:10.2136/sssaj2004.3940, 2004.*

[23] R1, P4, L140: mention ±0.01 and ±0.03 are uncertainties.

Added.

P4-5, L144-147: Thus, the HP measures real and imaginary soil permittivities (*uncertainties of* ± 0.2 or ± 1%, whichever is greater) as well as temperature (± 0.3°C). From these two variables, soil moisture is estimated using an empirical relationship calibrated for the given soil type (*uncertainties* between ± 0.01 and 0.03 volumetric water content depending on soil type), with…

[24] R1, P6, L185: It confused me whether the samples were collected from the temperature chamber or from the sites. It is the latter I understand? Further, I propose to use distinguishing names. Call the PVC boxes with the collected soil 'samples' as is, but refer to the cardboard boxes, filled with samples and surrounding sand, with a different name. Maybe sample assembly. Indicate these names in Figure 3. This way you can mention for example that the "sample assemblies were placed in the temperature chamber and were subjected to 3 (? mention this as well) freeze/thaw cycles".

Clarifications were added about the distinction between the collection of the samples at the study sites and the freeze/thaw cycles experiment in the temperature-controlled chamber. The components of the sample assembly were identified in Fig. 3. The soil samples underwent 2 or 3 freeze/thaw cycles, which is now specified.

P6, L204-206: Continuous permittivity measurements were conducted on the mineral and organic soil samples going through *two or three* consecutive freeze/thaw cycles in a NorLake2 mini-room walk-in controlled temperature-controlled chamber…

P6, L207-209: The soil samples *were previously collected from their respective study sites (see Sect. 3.2)* in PVC or plastic containers. *The OBS sample was collected using a rectangular container, while the other samples were collected using cylindrical containers.*

Fig. 3: Updated in manuscript.

[25] R1, P7, L243 – 246. Authors state that trends of OECP and HP are "very similar" and the fully frozen/thawed epsilon values are "also similar". I disagree with this description. Judging from Figures 5 - 8 there are significant differences. These differences and explanations for their causes are discussed further down in the text.

The similarity mentioned here was meant to point at the closer similarities between OECP and HP measurements than the model estimates. Since the model results are discussed in the next section, the sentence was reformulated to remove this mention.

P9, L294-296: The HP measurements show trends *in agreement with that of* the OECP measurements during freeze/thaw transitions, especially for the real permittivity*, although the fully* frozen and thawed permittivity values *display soil type dependent offsets* between the OECP and HP measurements (Tables 2 and 3).

[26] R1, P7, L251: ".. the freeze/thaw transition measurements are smoother with the HP than… " Perhaps there is a better alternative for "smoother", perhaps "less abrupt"? Also sentence should be "We also observe that the measured freeze/thaw transitions are less abrupt (?) with the measurements of the HP than with the OECP." Same for line 261.

The term ‘’smooth’’ was replaced through the manuscript by the terms ‘’steeper’’, ‘’continuous’’ and ‘’extended’’ depending on the context.

P5, L167-169: Zhang's model evaluates the unfrozen water fraction (f_w) in soil near the freezing point in order to obtain a continuous transition between the solid and liquid phases of water.

P9, L310: It can also be observed that the freeze/thaw transition measurements are *steeper* with the *OECP* than the *HP*.

P9, L311-313: Since the instruments measure an average permittivity for the whole probed volume, a larger probed volume will record a *more extended* freeze/thaw transition because of the longer time required for the freezing/thawing fronts to penetrate the depth of volume probed.

P9, L320-321: Zhang's model estimates the ice fraction for a given sub-freezing temperature, displaying a *continuous* freeze/thaw transition.

P11, L374-376: Based on our simulations, ice fraction representation in Zhang's model results in a more physically appropriate representation of processes around the freezing point and results in *freeze/thaw* transitions *closer to observations*.

[27] R1, P10, L325 - 327: The question whether the OECP correctly measures the epsilon in not shown in this manuscript. It is implied by your earlier work, see also comment [10].

The reliability of OECP measurements are not thoughtfully investigated in this study, although confidence in the reliability of the measurements can be inferred from the repeatability through freeze/thaw cycles. The conclusion was adapted to shift focus from OECP reliability to soil permittivity results and a hint to OECP measurements repeatability was added in the Results section.

P8, L281-282: *The repeatability of the OECP measurements can also be seen as an indicator of the reliability of the measurements.*

P11, L387-392: *This study presents soil microwave permittivity measurements during freeze/thaw transitions in* the same frequency range as the SMAP and SMOS satellites, as well as future L-band satellite missions. *The permittivity measurements were taken using a novel open-ended coaxial probe (OECP).* It is shown that lower frequency (MHz) soil permittivity probes can be used to estimate microwave permittivity given proper calibration relative to an L-band probe*, which holds significant potential considering the already widespread operational networks of low frequency soil permittivity probes deployed to measure soil moisture.*

[28] R1, Fig. 5 – 8: To make comparison easier I propose to let all figures have the same axis limits for epsilon' and epsilon", even if this implies having only one figure per page. Further I would recommend using more contrasting colours for the curves and to plot the graphs in vector format (PDF).

The color palette of figures 5 to 8 was changed to increase color contrast. The authors would prefer to stay with variable y-axis since the data from figure 7 would be hardly visible if put at the same scale of figure 8 (i.e. it would occupy a third of the graph for in the real permittivity graph and a sixth in the imaginary permittivity graph).

Figures 5-8: Updated in manuscript.

[29] R1, Tables 2 and 3: Besides the absolute uncertainty also indicate the relative uncertainty.

Relative uncertainties were added aside absolute values in Table 2 and 3.

Table 2: … *Absolute and relative* uncertainties (in parentheses) are based on instrument precision and measurement variability.

Table 2 and 3: Updated in manuscript.

Reviewer #2:

Synopsis:

The manuscript by Mavrovic et al. conducted permittivity measurements of different soil types with various soil water content using OECP and HydraProbe at frequency of L-band and 50MHz, respectively. Two experiments, fast freeze/thaw transition and slow freeze/thaw transition, were designed. Two soil dielectric model, TD GRMDM and Zhang's model, were driven by the known inputs to simulate the real and imaginary part of soil permittivity. By comparing permittivity measurements between OECP and HydraProbe during freeze/thaw cycles, they demonstrated there are differences of permittivity characteristic between L-band and MHz instruments and suggested the necessities to make proper calibration. By comparing the permittivity measurements and model simulations, they reported the observable discrepancies and highlighted the need for soil dielectric models to take into account the hysteresis effect. Such work is under the research topic to evaluate satellite microwave data products from the in situ permittivity measurements (MHz frequency).

The topic of this manuscript is of interest to the readers of HESS and the measurements can be potentially of importance to the microwave related researches. However, in its current form, the uncertainties regarding the measurements are not detail, which make it hard to judge the validity of the comparison of OECP and HydraProbe measurements. The difference between OECP and HydraProbe measurements is not only from the frequency dependence of permittivity, but also can come from the fact that they are not measuring the same volume of soil samples. As the temperature range of this experiment is large, the temperature dependence of OECP and HydraProbe measurements matters. In addition, the presentation of results is with inaccuracies and can be further explained. Given the current form of the manuscript, I cannot recommend its publication. I expect it suitable for publication in HESS with convinced presentation of measurements and results. Please see below my specific comments.

We made substantial improvement to the manuscript by adding a more explicit presentation of the OECP uncertainties and calibration dependency on temperature. Clarifications were also added on the impact of the temperature sensing volume versus the permittivity sensing volume on the hysteresis amplitude. The Results section was restructured with added explanations on the permittivity measurements. Details were added on the models' equations and assumptions.

Specific comments:

[1] R2, P1, Title and Abstract: I can not see any details about the description of soil dielectric characterization in the Abstract. Please consider either adjust the title or adding the relevant text in Abstract.

The title was adjusted to better reflect the study objectives.

P1, Title: Soil dielectric characterization during freeze-thaw transitions *using L-band coaxial probe and soil moisture probes*

[2] R2, P2, L71: "The high uncertainties in soil permittivity models result from the difficulty in gathering in situ permittivity…" as from my understanding, the uncertainties in soil permittivity models can come from the parameters is not well defined by the in situ permittivity measurements. please clarify this sentence.

The sentence was rewritten to clarify the impact of the lack of reliable microwave permittivity measurements on model parameterization and validation.

P2-3, L74-76: The difficulty in gathering *in situ* permittivity data at microwave frequencies *represents a major hindrance in the parameterization and validation of soil permittivity models, which induces high uncertainties in soil permittivity estimates*.

[3] R2, P3-4, L104 and L130: Section numbers are incorrect.

Corrected.

P4, L108: 2.1.1 Open-Ended Coaxial Probe (OECP)

P4, L134: 2.1.2 HydraProbe

[4] R2, P4, L124: please explain the temperature dependence of OECP measurements. As OECP undergoes a large variation of temperature (e.g., -10°C to 10°C), how does OECP perform under such conditions? At which temperature OECP is calibrated? Please make a clarification.

Details were added about the calibration of the OECP in this experiment. Since the OECP is an instrument in development, the calibration of the instrument is undertaken as frequently as possible, although there is a small temperature dependency, it was smaller than the measurement uncertainties. Commercial instruments, such as HydraProbes, are typically judged to have a calibration stable enough to have confidence in the manufacturer calibration throughout the temperature range.

P7, L220-228: *The OECP was calibrated (see Sect. 2.1.1) in the temperature-controlled chamber at +10°C. The OECP can operate at a wide range of temperature and was tested to temperature down to -30°C in the Canadian Arctic (Mavrovic et al., 2020). Beside the OECP, the Planar R54 reflectometer (Copper Mountain Technologies) generating and measuring the electromagnetic waves is graded for [-10 +50] °C temperature range and the Pasternack coaxial cable joining the OECP and the*

reflectometer for [-50 +205] °C temperature range. The OECP calibration displays a slight temperature dependency, where the calibration drift showed a 0.5% increase in permittivity when using a calibration at -15 °C compare to a calibration at 10 °C. This calibration drift is small compared to the measurement uncertainties (±3.3% for real permittivity and ±2.5% for imaginary permittivity; Mavrovic et al., 2018).

[5] R2, P5, Sect. 2.2: please consider presenting the equations used for TD GRMDM and Zhang's model, maybe can put in the appendix. As later you proposed a modification of Zhang's model to consider the hysteresis effect, It is better to present the equations and clear introduce how you make modifications.

Substantial details were added on the Zhang's model and TD GRMDM used for this study. The modifications to Zhang's model that were made to produce fig. 10 were explained in the response to comment R2[14].

P5-6: The order of Sections 2.2.1 and 2.2.2 were interchanged.

P5, L156-179: The model from Zhang et al. (2010) (henceforth Zhang's model) is a semi-empirical soil model for estimating microwave soil permittivity from soil physical characteristics. It is an extension of the semi-empirical mixing dielectric model (SMDM) adapted to frozen soils from Dobson et al. (1985). *Zhang's model is based on dielectric mixing for soil/air/water mixture to estimate soil permittivity at microwave frequencies:*

$$\varepsilon^{\alpha} = f_s\varepsilon_s^{\alpha} + f_a\varepsilon_a^{\alpha} + f_{fw}\varepsilon_{fw}^{\alpha} + f_{bw}\varepsilon_{bw}^{\alpha} + f_i\varepsilon_i^{\alpha} \quad (1)$$

where $\boldsymbol{\varepsilon}$ is the permittivity of the overall soil mixture, $\boldsymbol{\alpha}$ a constant shape factor (optimized at 0.65 by Zhang et al., 2003), f the fraction of each component in the soil mixture and the subscripts s, a, i, fw and bw refer respectively to solid soils, air, ice, free water and bound water. The approximation of combining free and bound water is made in the model to avoid evaluating the challenging bound water permittivity ($\boldsymbol{\varepsilon}_w$). Also, air contribution to permittivity is negligible ($\boldsymbol{\varepsilon}_a \approx 1$). Zhang's model evaluates the unfrozen water fraction (f_w) in soil near the freezing point in order to obtain a continuous transition between the solid and liquid phases of water. An empirical exponential decay function ($f_w = A \cdot |T_{soil}|^{-B}$) is used to estimate the liquid water vs. ice fractions in the freezing soils. The parameters A and B of the previous function were empirically estimated based on soil types (Zhang et al., 2003). *Solving eq. 1 to obtain an expression for soil mixture permittivity from constant and measurable parameters, Zhang et al. (2010) obtained:*

$$\varepsilon^{\alpha} = 1 + \frac{\rho_b}{\rho_s}(\varepsilon_s'^{\alpha} - 1) + f_w^{\beta}\varepsilon_w^{\alpha} - f_w + f_i\varepsilon_i^{\alpha} - f_i \quad (2)$$

where ρ_b represents soil bulk density, ρ_s soil specific density and β is a parameter that depends on soil composition. The input parameters required by Zhang's model *to evaluate all variables in eq. 2* include frequency (set at 1.4 GHz for this study), soil moisture (main driver for soil permittivity), temperature, dry bulk density and composition (clay, silt and sand fractions) (Zhang et al., 2003 and 2010; Mironov, 2017).

P6, L182-183: The TD GRMDM is a semi-empirical model that estimates the microwave permittivity of a soil from its physical properties *using a mixing dielectric approach similar to Zhang's model* (Mironov et al., 2010).

P6, L186-189: *The computational implementation of the TD GRMDM used in this experiment was provided by members of the CESBIO team (Centre d'Etudes Spatiales de la Biosphère, Toulouse, France) that worked on the operational product of the SMOS mission which used TD GRMDM as one of its modelling components.*

[6] R2, P6, L193: what is HPP?

The HPP was not used in this experiment, the reference was removed.

P7, L230: HP output signals were logged with a CR800 datalogger (Campbell Scientific, Inc.).

[7] R2, P6, Sect. 3.1.2: Slow freeze/thaw transition Please explain the purpose for this experiment. Please describe the temperature settings and add information about the measuring interval of OECP and HP measurements.

The purpose of the slow freeze/thaw transition is to observe the effect of transition speed on the amplitude of the hysteresis effect. This precision was added along with details on the temperature settings and variable measurement interval. It should be noted that no HP measurements were taken during the slow freeze/thaw transition experiment.

P7, L240-251: To investigate the effect of *a slower freeze/thaw transition on the temperature amplitude of the hysteresis effect,* another experimental setup was created in a Climats EXCAL 1411-HE cold chamber (0.138 m^3 volume) at the Laboratoire de l'Intégration du Matériau au Système (Bordeaux, France). Since the soil sample and the Polytetrafluoroethylene (i.e. PTFE or TEFLON) container had smaller volumes, the OECP probe was installed on top of the soil sample with its open end in contact with the soil (Fig. 4). Only OECP permittivity measurements were taken in this experiment since an HP sensor was not available. The objective of this experimental setup was to *experiment* a slow freeze/thaw transition. *Measurements were made to cover a soil temperature range from -20°C to +11.5°C with a variable soil temperature measurement interval to have a finer curve resolution around freezing point.* Permittivity measurements were taken only when the soil temperature equilibrated with the cold chamber air temperature (± 0.1°C). This method was significantly more time-consuming than the fast transition setup, as a full cycle took several days and required heavy user surveillance.

[8] R2, P6-7, Sect. 3.2: Maybe I have misunderstandings here. How many soil samples were collected and then used in this experiment? Are these soil samples for each site with the same moisture content?

The OBS soil sample consists of one sample in which all probes can properly fit. Two samples were used from the three other sites, one for the OECP and another for the HP. Explanations were added on the reason why two distinct setups were used which should enlighten the reader, see response to comment R1[2]. All soil samples were conserved as close as possible to their original moisture content as collected on the field. Those moisture content levels can be found in Table 1.

[9] R2, P7, L221: When is the experiment conducted?

Specified.

P8, L261: The samples were collected January *27th*, 2018.

Fig. 5: *Experiment conducted from February 1st to February 7th, 2018.*

Fig. 6: *Experiment conducted from April 15th to April 19th, 2018.*

Fig. 7: *Experiment conducted from March 29th to April 6th, 2018.*

Fig. 8: *Experiment conducted from April 6th to April 15th, 2018.*

Fig. 11: during a slow freeze/thaw cycle in a *temperature-controlled* chamber environment. *Experiment conducted July 12th, 2017.*

[10] R2, P7-8, Sect. 4: In this section, Figures 5-8 are presented. While only a general description was presented. Lacking of the characteristic of soil dielectric, the difference among Figures 5-8, the difference between fast and slow freeze/thaw transition measurements.

The Experimental Results section (4) was restructured for clarity. More details were added on the description of Figs. 5-8 and Table 2-3. Some comments were also added on the difference between the fast and slow freeze/thaw transitions.

P8-9, L279-315: Figures 5 to 8 show the complex permittivity of the four soil samples when undergoing consecutive *fast* freeze/thaw cycles. Of note, the freeze/thaw transitions were reproducible between cycles using both HP and OECP sensors. *The repeatability of the OECP measurements can also be seen as an indicator of the reliability of the measurements. Both thawed soil permittivity from the OECP (ε'_{thawed} = [6.5;22.8], ε''_{thawed} = [1.43;5.7]) and HP (ε'_{thawed} = [6.2;21.7], ε''_{thawed} = [1.7;10.0]) in Table 2 show a strong correlation between permittivity measurement and volumetric liquid water content as expected. For frozen soils (Table 3), the OECP (ε'_{frozen} = [3.5;6.0], ε''_{frozen} = [0.46;1.2]) and HP (ε'_{frozen} = [2.4;7.0], ε''_{frozen} = [0.47;2.8]) permittivity measurements do not seem to display any direct relationship with ice fraction or dry bulk density. Hysteresis effects can be observed between the freezing and thawing cycles in Figs. 5 through 8. Although hysteresis is reported in soil freezing studies, this effect was amplified by the temperature transition speed and differences in the sensing volume for*

temperature and permittivity observations (Pardo Lara et al.; 2020). *Fig. 11 shows a slow freeze/thaw transition displaying a hysteresis effect of diminished amplitude, but still noticeable. The explanation of the freeze/thaw hysteresis effect is further discussed in sect. 5 to highlight the respective impact of the temperature transition speed and the sensing volume of the temperature measurements versus the permittivity measurements.* The HP measurements show very similar trends to the OECP measurements during freeze/thaw transitions, especially for the real permittivity, *although the fully* frozen and thawed permittivity values *display soil type dependent offsets* between the OECP and HP measurements (Tables 2 and 3). The OECP and HP permittivity measurements, compared in the scatterplot of Fig. 9, are similar for the real part (RMSE = 1.03) but show larger discrepancies for the imaginary part (RMSE = 1.82). *Across soil types, no systematic bias between OECP and HP real permittivity were observed, although HP imaginary permittivity measurements tend to be systematically higher than OECP measurements, with the trend being more pronounced at higher imaginary permittivity (i.e. at higher liquid water content). It was expected that the* OECP measured imaginary *permittivity would be* lower than that of the HP because the dielectric loss due to liquid water is more pronounced *at L-band (OECP) than in the MHz frequencies* (Mätzler, 1987; Artemov and Volkov, 2014).

In most experiments presented, a short surge in permittivity can be observed right after thawing, followed by a small drop leading to a convergence to a relatively stable permittivity value associated with a fully thawed soil. Further investigation is needed to see if this short surge is due to water percolation through the soil sample toward the end of the thawing transition. It can also be observed that the freeze/thaw transition measurements are *steeper* with the *OECP* than the HP. This is partially due to the HP's larger probed volume. Since the instruments measure an average permittivity for the whole probed volume, a larger probed volume will record a *more extended* freeze/thaw transition because of the longer time required for the freezing/thawing fronts to penetrate the depth of volume probed. *More specifically, since the freezing/thawing front is mostly vertically oriented, it is the probes' volume diameter difference that cause the difference in transition steepness.*

[11] R2, P7, L242: please explain "Although hysteresis should be expected because of the latent heat of fusion of water".

See response to comment R1[3].

[12] R2, P7, L246: "with offsets depending on the soil type" please consider presenting the results more detail.

Details were added in this paragraph along with a reorganization of the flow of ideas. See response to comment R2[10].

[13] R2, P8, L267-268: "both models overestimated the soil permittivity of thawed samples with high water content according to the results of this study." please explain such overestimation.

It is hypothesized that the models' permittivity overestimation is due to an underestimation of bound water fraction or bound water permittivity. Evaluating the plausibility of this hypothesis is out of the scope of this study, further investigation would be required. This hypothesis was added to the Results section.

P10, L327-333: Lastly, both models overestimated the soil permittivity of thawed samples with high water content according to the results of this study (Fig. 5)*, which agrees with results from Bircher et al. (2016b). Further investigation would be required to identify the sources of permittivity overestimation in the models, although it is probable that it comes from the difficulty in uncoupled free and bound water in soil permittivity models. The movement of a fraction of water molecules under the soil surface is hindered by solid soil particles. Those constrained water molecules are described as bound water. Since their ability to align with an electrical field is reduced, the permittivity of bound water is reduced as well (Jones et al., 2002).*

P14, L516-517: *Jones, S., Wraith, J., and Or, D.: Time domain reflectometry measurement principles and applications, Hydrol. Process., 16(1), 141-153, doi: 10.1002/hyp.513, 2002.*

[14] R2, P9, L295: please consider presenting the equations of the modified version of Zhang's model.

As describe in the paragraph, the ice fraction was prescribed around freezing point in the Zhang's model using an exponential function ($\frac{e^x}{e^x+1}$). This is the only modification applied to the Zhang's model.

[15] R2, P9, L296: "consider ice fraction above 0ºC" is the artefact or the real conditions? Please make explanations.

This should be considered an artefact rather than real conditions, although this artefact is of relevant importance for soil permittivity applications (see response to comment R2[18]).

P10-11, L355-359: The classic Zhang's model only takes into account ice fraction below 0°C, *this ice fraction should not be interpreted as actual ice at temperature below freezing point but rather as an aggregate of the heterogeneous soil temperature.* Figure 10 demonstrates the hysteresis effect simulated by using a modified version of Zhang's model *that considers ice fraction above and below 0°C.*

[16] R2, P9, L300: please specify what is "the hypothesis".

See response to comment R1[8]

[17] R2, P9, L316: please explain how you implement a double "threshold"

Some additional explanation on the double threshold proposition was added.

P11, L376-385: To reproduce the hysteresis effect at freeze/thaw transition, two approaches are possible. An empirical approach could be used by implementing a double threshold *using distinct ice fraction empirical relationships for 1) the freezing and 2) the thawing cycle.* This empirical approach would require determining the freezing/thawing temperature offset independently for each transition type which would depend on liquid water content, textural composition, solute concentration, and the pore pressure of the soil (Daanen et al., 2011). The alternative would be to couple dielectric models with soil physical models that integrate the time evolution of soil physical properties (e.g. CLASSIC model; Melton at al., *2020*). Soil physical models provide an estimate of the ice fraction through time, which is used by dielectric models to estimate soil permittivity. Such coupling should only impact the freeze/thaw transition where ice fraction is a relevant parameter.

P15, L562-565: Melton, J., Arora, V., Wisernig-Cojoc, E., Seiler, C., Fortier, M., Chan, E., and Teckentrup, L.: CLASSIC v1.0: the open-source community successor to the Canadian Land Surface Scheme (CLASS) and the Canadian Terrestrial Ecosystem Model (CTEM) – Part 1: Model framework and site-level performance, Geosci. Model Dev., *13(6), 2825–2850, doi:10.5194/gmd-13-2825-2020, 2020.*

[18] R2, P10, Sect. 6: In the current form, conclusion appears not informative compared to the Abstract. Please consider making modifications, adding more information.

Modifications to the conclusion were made (see response to comment R1[27]) and information were added to the hysteresis effect implications.

P11, L395-397: *Although this phenomenon should be considered as an aggregate of soil temperature heterogeneity rather than actual conditions, it is of relevant interest to study and understand it for all macroscopic to satellite scale applications.*

[19] R2, P3, L95: considering change into “Section 2.2 gives an overview of two soil permittivity models”

Specified.

P3, L99-100: …Section 2.2 gives an overview of *two* soil permittivity models used for satellite retrieval…

[20] R2, Fig. 4: please add the plotting scale to indicate the dimensions.

Scale added in Fig. 4.

Fig. 4: Updated in manuscript.

[21] R2, Fig. 10: how is it reproduced? Please indicate the equations, the used parameters.

We updated and clarified the equations. For details on both the equations and parameters used, see response to comments R2[5] and R2[14]

[22] R2, Fig. 11: where are (a) and (b) on the figures?

Fig. 4 and 11 were joined in previous versions of the manuscript. Corrected.

Fig. 11: Real (ε') and imaginary (ε'') permittivity of an organic soil sample from the Old Black Spruce site (collected May 3rd, 2017) during a slow freeze/thaw cycle in a *temperature-controlled* chamber environment *(experiment conducted during July 2017)*.

[23] R2, Tables: Please consider using the consistent format

The tables' format was standardized.

Tables 1, 2 and 3: Updated in manuscript.

Reviewer #3:

Synopsis:

The manuscript presents interesting measurements of soil permittivity at L-band during the freeze-thaw cycles. Results are compared with two commonly used models (Mironov's model and Zhang's model) and hysteresis effects are observed especially for the fast freeze/thaw transitions. The reviewer found these experimental results are valuable and suggests to accept it for publication after addressing the following concerns.

Specific comments:

[1] R3, P2, L63-64: Not only for L-band, higher frequencies are also able to retrieve the land- scape freeze/thaw state. (e.g. Zuerndorfer et al., 1990; Judge et al., 1997; and Zhao et al., 2011). And if possible, future measurements could be extended to higher frequencies, which is important to retrieve snow properties and soil properties under the snow. Please refer to: Zuerndorfer, B. W., England, A. W., Dobson, M. C., & Ulaby, F. T. (1990). Mapping freeze/thaw boundaries with SMMR data. Agricultural and Forest Meteorology, 52(1-2), 199-225. Judge, J., Galantowicz, J. F., England, A. W., & Dahl, P. (1997). Freeze/thaw classification for prairie soils using SSM/I radiobrightnesses. IEEE Transactions on Geoscience and Remote Sensing, 35(4), 827-832. Zhao, T., Zhang, L., Jiang, L., Zhao, S., Chai, L., & Jin, R. (2011). A new soil freeze/thaw discriminant algorithm using AMSR-E passive microwave imagery. Hydrological Processes, 25(11), 1704-1716.

The authors acknowledge that the list of references for freeze/thaw soil state retrieval algorithm is long and cover a large range of microwave frequencies. Suggested references added.

P2, L66-68: This allows for the retrieval of the ground state (freeze/thaw) from passive microwave observations (*Zuerndorfer et al., 1990; Judge et al., 1997; Zhao et al., 2011*; Rautiainen et al. 2012; Roy et al., 2015; Derksen et al, 2017).

P14, L519-521: *Judge, J., Galantowicz, J., England, A., and Dahl, P.: Freeze/thaw classification for prairie soils using SSM/I radiobrightnesses, IEEE Trans. Geosci. Remote Sens., 35(4), 827-832, doi:10.1109/36.602525, 1997.*

P17, L687-689: *Zhao, T., Zhang, L., Jiang, L., Zhao, S., Chai, L., and Jin, R.: A new soil freeze/thaw discriminant algorithm using AMSR-E passive microwave imagery, Hydrol. Process., 25(11), 1704-1716, doi:10.1002/hyp.7930, 2011.*

P17, L691-692: *Zuerndorfer, B., England, A., Dobson, M., and Ulaby, F.: Mapping freeze/thaw boundaries with SMMR data, Agr. Forest Meteorol., 52(1-2), 199-225, doi:10.1016/0168-1923(90)90106-G, 1990.*

[2] R3, P4, L125: Would it cause uncertainties of measurement when applying different pressures to the soil with the OECP probe?

Yes, adding pressure to the probe would typically increase permittivity measurements because of the densification of the soil. On the other side, if the proper is not properly in contact with the soil, air gaps would produce artificially low permittivity measurements. There is a proper equilibrium to be found here, which is accomplished by digging a small-scale trench, alike soil moisture probes are generally installed in the field. The OECP is placed horizontally to position the probed volume in the undisturbed soil. The OECP is then fully buried to avoid air gap without risking of applying extra pressure. Precision was added about the installation method.

P6-7, L212-216: The OECP and HP were *horizontally inserted into undisturbed soil* and centered at a depth of 2.5 cm below the soil surface *with sufficient spacing between the probes and the soil samples edges to ensure that the probed volumes are restricted to the limits of the soil samples* (Fig. 3). *Special care was deployed to ensure no air gap was found between the OECP and the undisturbed soil, but without applying extra pressure on the probe.*

[3] R3, P7, L248: How are the data points selected for Figure 9, as there are many measurements as shown from Figure 5 to 8. The challenge is how to well model the soil permittivity during the freeze-thaw transitions, and data points during the freezing/thawing period should be included.

Data points of Fig. 9 are the displayed in Table 2 and 3 which represents stable plateau when the soil is fully frozen or thawed, from -6°C to -5°C or from +5°C to + 6°C

respectively. Fig. 9 allows for a comparison of measurements and modelling of soil permittivity away from the freeze/thaw transition, therefore values around freezing point and the hysteresis effect are avoided. Including data near the hysteresis would bias the results for the desired comparison aimed at with Fig. 9.

[4] R3, Fig. 9: please specify those numbers are for RMSE in the figure.

RMSE added in Fig. 9.

Fig. 9: Updated in manuscript.

[5] R3, P9, L290: It is very interesting that the hysteresis effects were observed during the permittivity measurement. As mentioned below by the authors, an empirical approach could be used by implementing a double threshold. It is suggested to do so to discuss the improvement of the model performance compared with results from Figure 9.

Some additional explanation on the double threshold proposition was added, see response to comment R2[17]. As for the implantation of such proposition in current soil permittivity models, this work will be reserved for future studies.

Soil dielectric characterization ~~at L-band microwave frequencies~~ during freeze-thaw transitions using L-band coaxial probe and soil moisture probes

Alex Mavrovic[1-2], Renato Pardo Lara[3], Aaron Berg[3], François Demontoux[4], Alain Royer[5-2], Alexandre Roy[1-2]

[1] Université du Québec à Trois-Rivières, Trois-Rivières, Québec, G9A 5H7, Canada
[2] Centre d'Études Nordiques, Université Laval, Québec, Québec, G1V 0A6, Canada
[3] University of Guelph, Guelph, Ontario, N1G 2W1, Canada
[4] Laboratoire de l'Intégration du Matériau au Système, Bordeaux, 33400 Talence, France
[5] Centre d'Applications et de Recherches en Télédétection, Université de Sherbrooke, Sherbrooke, Québec, J1K 2R1, Canada

Correspondence to: Alex Mavrovic (Alex.Mavrovic@uqtr.ca)

Abstract. Soil microwave permittivity is a crucial parameter in passive microwave retrieval algorithms but remains a challenging variable to measure. To validate and improve satellite microwave data products, precise and reliable estimations of the relative permittivity ($\varepsilon_r = \varepsilon/\varepsilon_0 = \varepsilon' - j\varepsilon''$; unitless) of soils are required, particularly for frozen soils. In this study, permittivity measurements were acquired using two different instruments: the newly designed open-ended coaxial probe (OECP) and the conventional Stevens HydraProbe. Both instruments were used to characterize the permittivity of soil samples undergoing several freeze/thaw cycles in a laboratory environment. The measurements were compared to soil permittivity models. ~~We show that the~~The OECP ~~is a suitable device for measuring~~measured frozen (ε'_{frozen} = [3.5;6.0], ε''_{frozen} = [0.446;1.2]) and thawed (ε'_{thawed} = [6.5;22.8], ε''_{thawed} = [1.443;5.7]) soil microwave permittivity. We also demonstrate that cheaper and widespread soil permittivity probes operating at lower frequencies (i.e. Stevens HydraProbe) can be used to estimate microwave permittivity given proper calibration relative to an L-band (1–2 GHz) probe. This study also highlighted the need to improve dielectric soil models, particularly during freeze/thaw transitions. There are still important discrepancies between *in situ* and modelled estimates and no current model accounts for the hysteresis effect shown between freezing and thawing processes which could have a significant impact on freeze/thaw detection from satellites.

Keywords: Open-ended coaxial probe, Freeze-thaw cycles, Soil permittivity, Microwave radiometry, Soil emission modelling

1 Introduction

The current generation of L-band (1–2 GHz) satellite-based radiometers offers a unique opportunity to monitor soil moisture and freeze/thaw cycles due to its global coverage and revisit time of only a few days (Kerr et al., 2012; Roy et al., 2015; Rautiainen et al., 2016; Colliander et al. 2017; Derksen et al., 2017; Wigneron et al., 2017). These satellites include the European Space Agency Soil Moisture Ocean Salinity mission (SMOS; Kerr et al., 2010), the National Aeronautics and Space Administration (NASA) Soil

Moisture Active Passive mission (SMAP; Entekhabi et al., 2010) and the NASA/CONAE (Comisión Nacional de Actividades Espaciales) joint Aquarius mission (Le Vine et al., 2010). Information about the physical state of the soil is retrieved from microwave observations by using radiative transfer models to simulate the interaction between electromagnetic waves and the surface. (Attema and Ulaby, 1978; Mo et al., 1982; Ulaby et al., 1990; Bracaglia et al., 1995; Huang et al., 2017). Such models have already been applied to obtain information on the characteristics of snow cover (Lemmetinen et al., 2016), the state of vegetation (Mo et al., 1982; Rodríguez-Fernández et al., 2018, Fan et al., 2018), soil moisture (Kerr et al., 2012; Mialon et al., 2015; Colliander et al. 2017) and soil freeze/thaw state (Kim et al., 2012; Rautiainen et al., 2016; Derksen et al., 2017; Roy et al., 2017a, 2018 and 2020; Prince et al., 2019).

Permittivities of the landscape constituents are crucial components of the dielectric models used to solve the electromagnetic equations governing the interaction between microwave and surface. The permittivity of a medium (ε, in F/m) determines its behavior when exposed to an electric field. The relative permittivity is the ratio between a medium's permittivity and that of a vacuum ($\varepsilon_r = \varepsilon/\varepsilon_0 = \varepsilon' - i\,\varepsilon''$; unitless; hereafter relative permittivity will stand for permittivity). Permittivity is characterized by a complex number, where the real part (ε') describes the ~~reorientation~~translation and rotation of molecular dipoles, which drives the wave propagation, and the imaginary part (ε'') describes the energy loss (absorption ~~(or loss) of energy.~~) associated with this process (Griffiths, 1999). The real and imaginary parts are linked through the Kramers–Kronig relations (Klingshirn, 2012), therefore they are not fully independent. A medium that strongly opposes the application of an external electric field displays a high permittivity (e.g. $\varepsilon'_{water} \approx 78–79$ in the 1–2 GHz frequency range; Pavlov and Baloshin, 2015) and a medium that does not strongly oppose an external electric field displays a low permittivity (e.g. $\varepsilon'_{air} \approx 1$).

Because of water's high permittivity, it dominates the microwave signal observed by satellite-based radiometers. Similarly, soil moisture retrieval algorithms exploit the high contrast in water-soil-air permittivity differences. However, the water phase also plays an important role in soil permittivity. When water freezes, the molecules become bound in a crystal lattice and the permittivity drops drastically compared to liquid water (i.e. $\varepsilon'_{ice} \approx 3$). The permittivity drop observable within freezing soils translates into a higher ~~passive~~ microwave emission from the ground. This allows for the retrieval of the ground state (freeze/thaw) from passive microwave observations (Zuerndorfer et al., 1990; Judge et al., 1997; Zhao et al., 2011; Rautiainen et al. 2012; Roy et al., 2015; Derksen et al, 2017). Soil permittivity is especially important in radiative transfer models since it acts as a boundary condition in the models. As microwave permittivity is challenging to measure in field settings, it is typically derived from empirical relationships and physical properties. Nonetheless, many uncertainties remain in the relationship between soil permittivity and soil physical parameters (Montpetit et al., 2018; Moradizadeh and Saradjian, 2016). This is especially evident during the winter when, in many cases, fixed values are introduced in data analysis algorithms due to a lack of better estimates or, in other cases, data are simply not available during winter. ~~The high uncertainties in~~

~~soil permittivity models result from the~~The difficulty in gathering *in situ* permittivity data at microwave frequencies ~~to parameterize~~represents a major hindrance in the parameterization and ~~validate these models~~validation of soil permittivity models, which induces high uncertainties in soil permittivity estimates. This is further complicated by the frequency dependence of permittivity.

Therefore, there is a need to collect better permittivity estimates for the validation of ~~passive~~ microwave ~~instruments~~observations and models. However, the majority of instruments deployed to validate microwave permittivity models, such as soil moisture sensors, use measurement frequencies (50–70 MHz) well outside the range of the concerned satellite observations (1400–1427 MHz). Until now, in the absence of a better alternative, the assumption that MHz and L-Band microwave soil permittivity are equivalent has been widely used to validate SMAP and SMOS algorithms (Roy et al., 2017a; Lemmetyinen et al., 2016), although this assumption was never rigorously tested. Furthermore, very few instruments used in field conditions continuously measure microwave permittivity in the frequency range of satellite sensors (Demontoux et al., 2019 and accepted). In addition, only a few laboratory studies have used L-Band permittivity measurements, and most of the available studies have focused on thawed soil samples (Bircher et a., 2016a and 2016b; Demontoux et al., 2017).

The goal of this laboratory-based study is to assess OECP L-band permittivity measurements in frozen soils and the implications of substituting them with permittivity estimates taken at lower frequency by: 1) evaluating the L-band permittivity of different types of soil in frozen and unfrozen conditions using an open-ended coaxial probe (OECP); 2) comparing the OECP measurements with those from a commercially available soil moisture ~~probe~~probes operating at a lower frequency (i.e. the Stevens HydraProbe) to evaluate the potential of these lower cost probes to estimate L-Band permittivity, and; 3) comparing the soil permittivity measurements captured with both devices against that predicted from soil permittivity models currently used in L-band passive microwave retrieval algorithms. This paper is structured as follows: Section 2.1 describes permittivity instruments used in this study; Section 2.2 gives an overview of two soil permittivity models used for satellite retrieval; Section 3 provides information on the study sites, data collection and laboratory setup. Lastly, in Sections 4 and 5, we compare and contrast the OECP measurements, commercial probe measurements and model simulations.

2 Theoretical background

2.1 Soil permittivity instruments

This study compares the permittivity estimates from two devices, an OECP and the Stevens HydraProbe, the following sections briefly describe these instruments.

2.~~2~~1.1 Open-Ended Coaxial Probe (OECP)

An OECP was developed by the Université de Sherbrooke (UdeS) and Université du Québec à Trois-Rivières (UQTR) to monitor the permittivity at L-band frequencies of tree trunks (Mavrovic et al., 2018) and snow (Mavrovic et al., 2020) (Fig. 1a). The OECP acts as a coaxial waveguide, and the reflection coefficient at the interface of its open edge and the probed medium is measured by a reflectometer connected to the OECP. This reflectometer acts as both ~~a~~an electromagnetic wave generator ~~providing electric field propagation to the probe~~ and a reflection coefficient measuring instrument for frequencies from 1 to 2 GHz. The reflection coefficient (i.e. magnitude of the reflected and incident electric field ratio) depends on the permittivity of the probed medium. The permittivity is retrieved from the reflection coefficient using a specific calibration based on open (air), short (copper plate) and standard samples (saline solutions of known permittivity) (Filali et al., 2006 and 2008). The permittivity of a wide range of materials can be measured by the OECP as long as it is possible to ensure the probe's open edge makes contact with a flat and smooth surface. This probe has already been described in detail and calibrated on known permittivity surfaces (Mavrovic et al., 2018 and 2020). The ~~penetration~~sensing depth of the OECP ~~can be~~is defined as the maximal depth at which a medium is ~~exposed~~polarized due to ~~a large enough~~the incident electric field ~~to be efficiently measured.~~, and as such contributes to the electromagnetic wave reflection. The ~~magnitude of this effective electric field in the medium~~sensing depth is proportional to the medium's permittivity and ~~depends on~~the magnitude of the electric field ~~magnitude~~ generated by the reflectometer, which ~~is~~displays a constant ~~(~~power output of 10 dBm~~)~~ (Fig. 1b). The OECP typical ~~penetration~~sensing depth approaches 1 cm under dry soil conditions and the cylindrical probed volume is about 3.5 cm wide in diameter (Figure 2). Under wet soil conditions, the ~~penetration~~sensing depth shrinks down to 0.4 cm. Under wet soil conditions, the sensing depth shrinks down to 0.4 cm. The probe system is operational in remote environments since it is easily transportable, sensibly sized (low weight and small dimensions), energy efficient, weatherproof, and operates at low temperatures. The OECP integrates a permittivity measurement in less than a second and does not require destructive sampling, although the user must be careful to avoid air gaps between the probe and the soil. While tested on reference solids, the OECP display uncertainties under 3.3% for real permittivity and under 2.5% or 0.04 (whichever is greater) for imaginary permittivity (Mavrovic et al., 2018).

2.1.2~~.1~~ HydraProbe

The HydraProbe (HP) is a commercial soil moisture probe, from *Stevens Water Monitoring Systems, Inc.,* that uses coaxial impedance dielectric reflectometry to measure soil permittivity (HydraProbes Soil Sensor User Manual, 2018). A digital model of the HP using the SDI-12 protocol was employed. The probe consists of a cylindrical casing which houses the electronics as well as four stainless steel tines (0.3 cm in diameter, 5.7 cm long) that protrude from a metal base plate (4.2 cm diameter). Three tines are arranged in a circle 3.0 cm in diameter around a central tine. The HP operates at 50 MHz and probes a larger volume than the OECP, ranging between approximately 40 and 350 cm^3. ~~Like the OECP, it uses the ratio of the incident and reflected waves to numerically solve Maxwell's equations, yielding the impedance and~~ The HP soil complex

permittivity. computation is derived from the impedance measurements between the steel tines, which depends mainly on the liquid water content of the soil surrounding the tines (Kraft et al., 1988, Campbell et al., 1988 and 1990, Seyfried et al., 2004). Thus, the HP measures real and imaginary soil permittivities (±(uncertainties of ± 0.2 or ± 1%, whichever is greater) as well as temperature (± 0.3°C). From these two variables, soil moisture is estimated using an empirical relationship calibrated for the given soil type (uncertainties between ± 0.01 and 0.03 volumetric water content depending on soil type), with individual calibrations resulting in slightly lower uncertainties (Seyfried et al., 2005; Burns et al., 2014; Rowlandson et al., 2013). This probe is widely used to measure soil moisture for meteorological and agricultural applications. It is deployed along several meteorological station networks (e.g Tetlock et al. 2019). Figure 2 illustrates typical probed volumes for the OECP (dry ~10 cm^3, wet ~5 cm^3) and HP (dry ~40 cm^3, wet ~350 cm^3) under dry and wet soil conditions.

2.2 Soil permittivity models

Two models commonly used in the remote sensing community for the retrieval of the soil freeze-thaw state were selected.

2.2.1 Zhang's Model

The model from Zhang et al. (2010) (henceforth Zhang's model) is a semi-empirical soil model for estimating microwave soil permittivity from soil physical characteristics. It is an extension of the semi-empirical mixing dielectric model (SMDM) adapted to frozen soils from Dobson et al. (1985). Zhang's model is based on dielectric mixing for soil/air/water mixture to estimate soil permittivity at microwave frequencies:

$$\varepsilon^{\alpha} = f_s\varepsilon_s^{\alpha} + f_a\varepsilon_a^{\alpha} + f_{fw}\varepsilon_{fw}^{\alpha} + f_{bw}\varepsilon_{bw}^{\alpha} + f_i\varepsilon_i^{\alpha} \quad (1)$$

where $\boldsymbol{\varepsilon}$ is the permittivity of the overall soil mixture, $\boldsymbol{\alpha}$ a constant shape factor (optimized at 0.65 by Zhang et al., 2003), *f* the fraction of each component in the soil mixture and the subscripts *s*, *a*, *i*, *fw* and *bw* refer respectively to solid soils, air, ice, free water and bound water. The approximation of combining free and bound water is made in the model to avoid evaluating the challenging bound water permittivity ($\boldsymbol{\varepsilon}_w$). Also, air contribution to permittivity is negligible ($\boldsymbol{\varepsilon}_a \approx 1$). Zhang's model evaluates the unfrozen water fraction (f_w) in soil near the freezing point in order to obtain a continuous transition between the solid and liquid phases of water. An empirical exponential decay function ($f_w = A \cdot |T_{soil}|^{-B}$) is used to estimate the liquid water vs. ice fractions in the freezing soils. The parameters A and B of the previous function were empirically estimated based on soil types (Zhang et al., 2003). Solving eq. 1 to obtain an expression for soil mixture permittivity from constant and measurable parameters, Zhang et al. (2010) obtained:

$$\varepsilon^{\alpha} = 1 + \frac{\rho_b}{\rho_s}(\varepsilon_s'^{\alpha} - 1) + f_w^{\beta}\varepsilon_w^{\alpha} - f_w + f_i\varepsilon_i^{\alpha} - f_i \quad (2)$$

where ρ_b represents soil bulk density, ρ_s soil specific density and β is a parameter that depends on soil composition. The input parameters required by Zhang's model to evaluate all variables in eq. 2 include frequency (set at 1.4 GHz for this study), soil moisture (main driver for soil permittivity), temperature, dry bulk density and composition (clay, silt and sand fractions) (Zhang et al., 2003 and 2010; Mironov, 2017).

2.2.2 Temperature Dependable Generalized Refractive Mixing Dielectric Model (TD GRMDM)

The TD GRMDM is a semi-empirical model that estimates the microwave permittivity of a soil from its physical properties using a mixing dielectric approach similar to Zhang's model (Mironov et al., 2010). The model accounts for the effect of soil granulometry, temperature and water liquid content through empirical relationships. This model allows for the distinction of bound and free water, giving each of these components a distinct dielectric spectrum. The computational implementation of the TD GRMDM used in this experiment was provided by members of the CESBIO team (Centre d'Etudes Spatiales de la Biosphère, Toulouse, France) that worked on the operational product of the SMOS mission which used TD GRMDM as one of its modelling components. The input parameters required in TD GRMDM are frequency (set at 1.4 GHz for this study), soil moisture, temperature, dry bulk density and clay fraction. Soil moisture is the main parameter driving soil permittivity. This model was built and validated on a soil database comprising the full range of textures covered by the SMOS mission (Mialon et al., 2015; Mironov et al., 2009 and 2010). However, with respect to the soil water freeze/thaw state, TD GRMDM is a binary model. All water in the soil is either thawed or frozen, therefore the freeze/thaw transition appears as a discontinuity. The model, however, allows for offsetting the freeze/thaw transition temperature to account for freezing point depression. TD GRMDM uses fixed values for frozen soils with no dependency on temperature, ice fraction or soil composition.

~~2.2.2 Zhang's Model~~

~~The model from Zhang et al. (2010) (henceforth Zhang's model) is a semi-empirical soil model for estimating microwave soil permittivity from soil physical characteristics. It is an extension of the semi-empirical mixing dielectric model (SMDM) adapted to frozen soils from Dobson et al. (1985). Zhang's model evaluates the ice fraction (f_i) in soil near the freezing point in order to obtain a smooth transition between the solid and liquid phases of water. An empirical exponential decay function ($f_i = A \cdot |T_{soil}|^{-B}$) is used to estimate the liquid water vs. ice fractions in the freezing soils. The parameters A and B of the previous function were empirically estimated based on soil type. From this ice fraction estimate, the approach uses semi-empirical dielectric mixing equations for soil water/ice mixture to estimate soil permittivity at microwave frequencies. The input parameters required by Zhang's model include frequency (set at 1.4 GHz for this study), soil moisture (main driver for soil permittivity), temperature, dry bulk density and composition (clay, silt and sand fractions) (Zhang et al., 2003 and 2010; Mironov, 2017).~~

3 Data and methods

3.1 Methods

Two experiments were performed in this study, the first under fast freeze/thaw transition conditions (one-time air temperature adjustment), and the second under slow transition conditions with small progressive increases in air temperature.

3.1.1 Fast freeze/thaw transition

Continuous permittivity measurements were conducted on mineral and organic soil samples going through ~~several~~two or three consecutive freeze/thaw cycles in a NorLake2 mini-room walk-in controlled temperature chamber (5.55 to 19.11 m^3 volume) equipped with a CP7L control panel at the School of Environmental Science of the University of Guelph (UofG). The soil samples were previously collected from their respective study sites (see Sect. 3.2) in PVC or plastic containers. The OBS sample was collected using a rectangular container, while the other samples were collected using cylindrical containers. The containers were placed in an insulated cardboard box (28x38x33 cm for a volume of $3.5x10^4$ cm^3) filled with sand to surround the soil samples (Fig. 3). This setup was intended to simulate the hot/cold front coming from the surface by isolating the sides and bottom of the soil samples. ~~The OECP and HP were fully buried and centered at a depth of 2.5 cm below the soil surface (Fig. 3).~~The OECP and HP were horizontally inserted into undisturbed soil and centered at a depth of 2.5 cm below the soil surface with sufficient spacing between the probes and the soil samples edges to ensure that the probed volumes are restricted to the limits of the soil samples (Fig. 3). Special care was deployed to ensure no air gap was found between the OECP and the undisturbed soil, but without applying extra pressure on the probe. The Fig. 3a and 3b setup discrepancies only reflect the two distinct containers used for soil collection at different sites, both configurations ensured sufficient spacing for undisturbed measurements. For the organic soil samples, into which multiple probes were inserted, sufficient spacing (~ 7.5 cm with the OECP and > 1 cm between the HP) between probes was ensured to avoid probe interaction. The OECP was calibrated (see Sect. 2.1.1) in the temperature-controlled chamber at +10°C. The OECP can operate at a wide range of temperature and was tested to temperature down to -30°C in the Canadian Arctic (Mavrovic et al., 2020). Beside the OECP, the Planar R54 reflectometer (Copper Mountain Technologies) generating and measuring the electromagnetic waves is graded for [-10 +50] °C temperature range and the Pasternack coaxial cable joining the OECP and the reflectometer for [-50 +205] °C temperature range. The OECP calibration displays a slight temperature dependency, where the calibration drift showed a 0.5% increase in permittivity when using a calibration at -15 °C compare to a calibration at 10 °C. This calibration drift is small compared to the measurement uncertainties (±3.3% for real permittivity and ±2.5% for imaginary permittivity; Mavrovic et al., 2018).

HP output signals were logged with a CR800 datalogger ~~and HPP output signals were logged with a CR1000 datalogger (both from~~ (Campbell Scientific, Inc.). Unlike the HP, the OECP does not record temperature. Therefore, a Campbell Scientific ~~107~~ temperature probe (model 107) was placed next to the OECP to measure

soil temperature. The air temperature of the cold chamber was set at +10°C for thawing cycles (initial air temperature of -10°C) and -10°C for freezing cycles (initial air temperature of +10°C). These experimental conditions allowed for a complete freeze/thaw cycle in approximately 24 hours and were chosen for practical considerations. However, it should be acknowledged that these conditions represent a relatively rapid transition. Permittivity and temperature measurements were set at one-minute intervals for all instruments.

3.1.2 Slow freeze/thaw transition

To investigate the effect of a slower ~~transitions~~freeze/thaw transition on the temperature amplitude of the hysteresis effect, another experimental setup was created in a Climats EXCAL 1411-HE cold chamber (0.138 m^3 volume) at the Laboratoire de l'Intégration du Matériau au Système (Bordeaux, France). Since the soil sample and the Polytetrafluoroethylene (i.e. PTFE or TEFLON) container had smaller volumes, the OECP probe was installed on top of the soil sample with its open end in contact with the soil (Fig. 4). Only OECP permittivity measurements were taken in this experiment since an HP sensor was not available. The objective of this experimental setup was to ~~force a slow freeze/thaw transition.~~experiment a slow freeze/thaw transition. Measurements were made to cover a soil temperature range from -20°C to +11.5°C with a variable soil temperature measurement interval to have a finer curve resolution around freezing point. Permittivity measurements were taken only when the soil temperature equilibrated with the cold chamber air temperature (± 0.1°C). This method was significantly more time-consuming than the fast transition setup, as a full cycle took several days and required heavy user surveillance.

3.2 Studied soil types

~~The studied~~Studied soil samples were collected from four different sites and consisted of a single homogenous soil layer (Table 1). Care was taken during transportation to the cold chamber to preserve their original state and leave their structure and moisture content as undisturbed as possible.

The first site was located in the boreal forest at the Old Black Spruce Research Station (OBS). This research facility is in northern Saskatchewan near Canada's boreal forest southern limit and is part of the Boreal Ecosystem Research and Monitoring Sites (BERMS). Its soil is rich in organic matter, displays high soil moisture levels for most of the thawed season (Gower et al., 1997), and is further described in Roy et al. (2020). The samples were collected ~~in~~ January 27th, 2018.

The remaining sites were all in agricultural fields with mineral soils in southern Ontario, Canada. Soil samples were collected at the University of Guelph's Elora Research Station (sandy loam; collected late fall 2017) as well as on private farms in Cambridge (loamy sand; collected late fall 2017) and Dunnville (clay loam; collected mid-winter 2018). The soils were selected to be representative of a range of soil textures and complement existing research at the three locations. These samples and their collection process are further

described in Pardo Lara et al. (2020) and the data are available at the Federated Research Data Repository through the Polar Data Catalog of metadata (PDC; https://dx.doi.org/10.20383/101.0200).

The soil composition and liquid water content of each sample were analyzed (Table 1). A particle size analysis of the OBS sample was completed at the UdeS using a soil sifting approach to determine the sand fractions and a densitometry technique based on Stokes law (Mériaux, 1953 and 1954) for the clay and silt fractions. The particle sizes of the Dunville, Elora and Cambridge samples were all measured using the hydrometer method (Bouyoucos, 1962). Liquid water content was measured using the drying and weighting technique for all soil samples (O'Kelly, 2004).

4 Results

4.1 Experimental results

Figures 5 to 8 show the complex permittivity of the four soil samples when undergoing consecutive fast freeze/thaw cycles. Of note, the freeze/thaw transitions were reproducible between cycles using both HP and OECP sensors. The repeatability of the OECP measurements can also be seen as an indicator of the reliability of the measurements. Both thawed soil permittivity from the OECP (ε'_{thawed} = [6.5;22.8], ε''_{thawed} = [1.43;5.7]) and HP (ε'_{thawed} = [6.2;21.7], ε''_{thawed} = [1.7;10.0]) in Table 2 show a strong correlation between permittivity measurement and volumetric liquid water content as expected. For frozen soils (Table 3), the OECP (ε'_{frozen} = [3.5;6.0], ε''_{frozen} = [0.46;1.2]) and HP (ε'_{frozen} = [2.4;7.0], ε''_{frozen} = [0.47;2.8]) permittivity measurements do not seem to display any direct relationship with ice fraction or dry bulk density. Hysteresis effects can be observed between the freezing and thawing cycles in Figs. 5 through 8~~.~~, i.e. a different behavior of permittivity variation depending on whether the ground freezes or thaws. Although hysteresis ~~should be expected because of the latent heat of fusion of water~~is reported in soil freezing studies, this effect was amplified by the ~~experimental setup and~~ temperature transition speed and differences in the sensing volume for temperature and permittivity observations (Pardo Lara et al~~.~~., 2020). ~~The HP measurements show very similar~~ Fig. 11 shows a slow freeze/thaw transition displaying a hysteresis effect of diminished amplitude, but still noticeable. The explanation of the freeze/thaw hysteresis effect is further discussed in sect. 5 to highlight the respective impact of the temperature transition speed and the sensing volume of the temperature measurements versus the permittivity measurements. The HP measurements show trends ~~to~~in agreement with that of the OECP measurements during freeze/thaw transitions, especially for the real permittivity~~. The~~ , although the fully frozen and thawed permittivity values ~~are also similar between the OECP and HP measurements, with offsets depending on the~~ display soil type dependent offsets between the OECP and HP measurements (Tables 2 and 3). The OECP and HP permittivity measurements, compared in the scatterplot of Fig. 9, are similar for the real part (RMSE = 1.03) but show larger discrepancies for the imaginary part (RMSE = 1.82). Across soil types, no systematic bias between OECP and HP real permittivity were observed, although HP imaginary permittivity measurements tend to be systematically higher than OECP

measurements, with the trend being more pronounced at higher imaginary permittivity (i.e. at higher liquid water content). It was expected that the OECP measured imaginary permittivity would be lower than that of the HP because the dielectric loss due to liquid water is more pronounced at L-band (OECP) than in the MHz frequencies (Mätzler, 1987; Artemov and Volkov, 2014).

~~The OECP and HP~~ In most experiments presented, a short surge in permittivity ~~measurements, compared in~~ can be observed right after thawing, followed by a small drop leading to a convergence to a relatively stable permittivity value associated with a fully thawed soil. Further investigation is needed to see if this short surge could be related to moisture migration toward the ~~scatterplots of Fig. 9, are similar for~~thawing front and to water percolation through the ~~real part (RMSE = 1.03) but show larger discrepancies for~~soil sample toward the ~~imaginary part (RMSE = 1.82). The OECP measured imaginary part is, as expected, lower than that~~end of the ~~HP because at microwave frequencies the dielectric loss due to liquid water is more pronounced (Mätzler, 1987; Artemov and Volkov, 2014).~~thawing transition. It can also be observed that the freeze/thaw transition measurements are ~~smoother~~steeper with the OECP than the HP ~~than the OECP.~~. This is ~~partially~~probably due to the HP's larger probed volume. Since the instruments measure an average permittivity for the whole probed volume, ~~a~~the larger probed volume ~~will record a smoother~~of the HP records an extended freeze/thaw transition because of the longer time required for the freezing/thawing fronts to penetrate the depth of volume probed. Since the freezing/thawing front is mostly vertically oriented, it is the difference in probes' sensing diameter that causes the difference in transition steepness.

4.2 Model Results

Soil parameters from Table 1 were used to drive the TD GRMDM and Zhang's model. Output from the models is shown in Figs. 5 to 9 and summarized in Tables 2 and 3. There are important discrepancies between the data and the models. The TD GRMDM does not simulate the freeze/thaw transition, resulting in a discontinuity in soil permittivity at the freezing point. Zhang's model estimates the ice fraction for a given sub-freezing temperature, displaying a ~~smoother~~continuous freeze/thaw transition. Even if amplified by the experimental setup, the hysteresis effect between the freezing and thawing cycles is not simulated by any model since they do not ~~consider latent heat.~~include the evolution of soil properties in time. The divergence between models and data is more prevalent for the imaginary part of the permittivity than for the real part. Zhang's model seems to systematically underestimate frozen soil permittivity, while the TD GRMDM fixed value approach is closer to the measured permittivity although it does not account, when the soil is frozen, for soil composition or ice content. Lastly, both models overestimated the soil permittivity of thawed samples with high water content according to the results of this study~~.~~ (Fig. 5), which agrees with results from Bircher et al. (2016b). Further investigation would be required to identify the sources of permittivity overestimation in the models, although it is probable that it comes from the difficulty in uncoupled free and bound water in soil permittivity models. The movement of a fraction of water molecules under the soil surface is hindered by solid soil particles. Those constrained water molecules are described as bound water. Since their ability

to align with an electrical field is reduced, the permittivity of bound water is reduced as well (Jones et al., 2002).

5 Discussion

The temperature dependence trend of permittivity during freeze/thaw transitions was similar across almost all OECP and HP measurements. The main difference between the permittivity measured at microwave and MHz frequencies appears to be an offset dependent on the soil type. Therefore, based on the offsets seen in Tables 2 and 3 and Fig. 9, a calibration equation between L-band and MHz permittivity can be obtained for a given soil. This would allow for the use of low-cost and widespread instrumentation in the MHz spectrum, such as the HP, to act as surrogate L-band soil permittivity measurements. This opens up the possibility of studies over large areas through already deployed networks. It should be remembered that MHz permittivity measurements have already been used to ~~validate~~test SMAP and SMOS algorithm's permittivity under the assumption that the MHz and L-band permittivity are equivalent (Roy et al., 2017a; Lemmetyinen et al., 2016). As our results showed, MHz and L-band soil permittivity trends are close to each other but not identical, therefore the previous assumption must be reconsidered because neglecting the frequency dependence of soil permittivity induces a bias in the results.

~~An important consideration in the use of devices for measuring the soil permittivity is the sample volume of the measurement. The HP and OECP instruments vary with respect to the soil volume probed. Ground-based~~Ground and satellite-based L-band radiometric measurements are very sensitive to the freezing of the first ~~centimetre~~centimeter of soil (Rowlandson et al., 2018; Roy et al., 2017a ~~and 2017b~~, b; Williamson et al., 2018). Therefore, the shallower depth (~ 0.4–1 cm) and smaller volume (~4–10 cm^3) probed by the OECP makes it a potentially more suitable instrument to study ~~and understand~~ the freeze/thaw signal observed from L-band radiometers.

The hysteresis effect observed in Figs. 5 to 8 was likely amplified by the experimental setup because of the fast temperature transition speed used. Nonetheless, the hysteresis effect is expected to occur because of the asymmetry between the freezing and thawing processes. The ~~hysteresis is partially explained by the latent heat of fusion of water, that is to say that the soil does~~classic Zhang's model only takes into account ice fraction below 0°C, this ice fraction should not ~~start to freeze until the~~be interpreted as actual ice at temperature ~~is~~ below freezing point ~~and does not thaw until the~~ but rather as an aggregate of the heterogeneous soil temperature ~~is over 0°C~~. Figure 10 demonstrates the hysteresis effect simulated by using a modified version of Zhang's model~~. The classic Zhang's model only takes into account ice fraction below 0°C. Zhang's model was modified to consider~~ that considers ice fraction above and below 0°C. This ice fraction was prescribed following an exponential function ($\frac{e^x}{e^x+1}$) around the freezing point. For a proper

estimation of ice fraction in soil, the evolution of the soil and boundary conditions should be simulated using more complex models like CLASSIC (Melton at al., ~~in review~~2020).

~~This hypothesis was tested on~~We further tested the hypothesis that the hysteresis effect is correlated with the temperature transition speed using an OBS soil sample using a slower freeze/thaw transition rate. The hysteresis effect displayed in Fig. 11 is still noticeable (< 1°C offset from freezing point) but not as pronounced as in Figs. 5 to 8 (between 2°C and 3°C offset from freezing point). Since the soil permittivity has an important impact on brightness temperature as observed by satellite-based radiometers (Roy et al., 2017a and 2017b; Jonard et al., 2018; Prince et al., 2019~~; Jonard et al., 2018),;),~~ it is notable that this hysteresis effect around freezing point is not taken into account in current soil models used in microwave satellite retrieval algorithms. The omission of this effect may potentially have an impact on freeze/thaw detection products and their validation. It should be noted that this hysteresis effect is not always observed for *in situ* data due to the instrumental uncertainty not being precise enough to conclusively separate the hysteresis effect *in situ* (e.g. Pardo Lara et al., 2020). The effect might also be mitigated at the pixel scale of modern satellites because of spatial heterogeneity (Roy et al. 2017b).

Based on our simulations, ice fraction representation in Zhang's model results in a more physically appropriate representation of processes around the freezing point and results in ~~smoother~~freeze/thaw transitions closer to observations. It should be noted that an ice fraction could be implemented in TD GRMDM as well. To reproduce the hysteresis effect at freeze/thaw transition, two approaches are possible. An empirical approach could be used by implementing a double threshold ~~(variable~~using distinct ice fraction empirical relationships for 1) the ~~freeze~~freezing and 2) the ~~thaw~~thawing cycle~~).~~. This empirical approach would require determining the freezing/thawing temperature offset independently for each transition type which would depend on liquid water content, textural composition, solute concentration, and the pore pressure of the soil (Daanen et al., 2011). The alternative would be to couple dielectric models with soil physical models that integrate the time evolution of soil physical properties (e.g. CLASSIC model; Melton at al., ~~in review~~2020). Soil physical models provide an estimate of the ice fraction through time, which is used by dielectric models to estimate soil permittivity. Such coupling should only impact the freeze/thaw transition where ice fraction is a relevant parameter.

6 ~~Conclusions~~Conclusion

~~The~~This study ~~shows that the open-ended coaxial probe (OECP) is a suitable device for measuring~~presents soil microwave permittivity measurements during freeze/thaw transitions in the same frequency range as the SMAP and SMOS satellites, as well as future L-band satellite missions. ~~We also showed~~The permittivity measurements were taken using a novel open-ended coaxial probe (OECP). It is shown that lower frequency (MHz) soil permittivity probes can be used to estimate microwave permittivity given proper calibration relative to an L-band probe~~.~~, which holds significant potential considering the already widespread operational

networks of low frequency soil permittivity probes deployed to measure soil moisture. This study also highlighted the need to improve dielectric soil models, particularly during freeze/thaw transitions. We observed noticeable discrepancies between *in situ* data and model estimates, and no current model accounts for the hysteresis effect shown between freezing and thawing processes. Although this phenomenon should be considered as an aggregate of soil temperature heterogeneity rather than actual conditions, it is of relevant interest to study and understand it for all macroscopic to satellite scale applications. Few studies have investigated this hysteresis effect, which could have a significant impact on freeze/thaw detection from satellites. Future work will look to improve soil thermal regime retrieval near the freezing point using permittivity measurements, which is impactful on the evaluation of the carbon budgets of northern regions.

7 Acknowledgments

This work was made possible thanks to the contributions of the Canadian Space Agency (CSA), Natural Sciences and Engineering Research Council of Canada (NSERC), Canada Foundation for Innovation (CFI). The experiments in Bordeaux were supported by the Samuel-De-Champlain France-Québec collaborative project (Fonds québécois de la recherche sur la nature et les technologies, FQRNT). We would also like to thank Bilal Filali, PhD, for his contribution to the design and manufacture of the probe, along with Simone Bircher, Arnaud Mialon, Yann Kerr and the entire CESBIO team in Toulouse for their contributions to probe testing and collaboration with Bordeaux laboratory. A special thanks to Jean-Pierre Wigneron from INRA for providing the codes to run the TD GRMDM model.

8 Competing interests

The authors declare that they have no conflict of interest.

9 Data availability

The research data can be accessed by direct request to the author.

References

Artemov, V., and Volkov, A.: Water and Ice Dielectric Spectra Scaling at 0°C, Ferroelectr., 466, 158–165, https://doi.org/:10.1080/00150193.2014.895216, 2014.

Attema, E., and Ulaby, F.: Vegetation modeled as a water cloud. Radio Sci., 13(2), 357-364, doi:10.1029/RS013i002p00357, 1978.

Bircher, S., Anreasen, M., Vuollet, J., Vehviläinen, J., Raitiainen, K., Jonard, F., Weihermüller, L., Zakharova, E., Wigneron, J.-P., and Kerr, Y.: Soil moisture sensor calibration for organic soil surface layers, Geosci. Instrum. Methods Data Syst., 5, 109–125, https://doi.org/:10.5194/gi-5-109-2016, 2016a.

Bircher, S., Demontoux, F., Razafindratsima, S., Bircher, S., Zakharova, E., Drusch, M., Wigneron, J.-P., and Kerr, Y.: L-Band Relative Permittivity of Organic Soil Surface Layers—A New Dataset of Resonant Cavity Measurements and Model Evaluation, Remote Sens., 8, 1024, https://doi.org/:10.3390/rs8121024, 2016b.

Bracaglia, M., Ferrazzoli, P., and Guerriero, L.: A fully polarimetric multiple scattering model for crops, Remote Sens. of Environ., 54(3), 170–179, doi:10.1016/0034-4257(95)00151-4, 1995.

Burns, T., Adams, J., and Berg, A.: Laboratory Calibration Procedures of the Hydra Probe Soil Moisture Sensor: Infiltration Wet-Up vs. Dry-Down, Vadose Zone J., 13(12), 1–10, https://doi.org/:10.2136/vzj2014.07..0081, 2014.

Bouyoucos, G.: Hydrometer method improved for making particle size analysis of soils, Agron. J., 54(5), 464–465, https://doi.org/:10.2134/agronj1962.00021962005400050028x, 1962.

Campbell, J.: Dielectric Properties and Influence of Conductivity in Soils at One to Fifty Megahertz, Soil Sci. Soc. Am. J., 54(2), 332-341, doi:10.2136/sssaj1990.03615995005400020006x, 1990.

Colliander, A., Jackson, T., Bindlish, R., Chan, S., Das, N., Kim, S., Cosh, M., Dunbar, R., Dang, L., Pashaian, L., Asanuma, J., Aida, K., Berg, A., Rowlandson, T., Bosch, D., Caldwell, T., Caylor, K., Goodrich, D., al Jassar, H., Lopez-Baeza, E., Martínez Fernández, J., González-Zamora, A., Livingston, S., McNairn, H., Pacheco, A., Moghaddam, M., Montzka, C., Notarnicola, C., Niedrist, G., Pellarin, T., Prueger, J., Pulliainen, J., Rautiainen, K., Ramos, J., Seyfried, M., Starks, P., Su, Z., Zeng, Y., van der Velde, R., Thibeault, M., Dorigo, W., Vreugdenhil, M., Walker, J. P., Wu, X., Monerris, A., O'Neill, P. E., Entekhabi, D., Njoku, E.G., and Yueha, S.: Validation of SMAP surface soil moisture products with core validation sites, Remote Sens. Environ., 191, 215-231, https://doi.org/:10.1016/j.rse.2017.01.021, 2017.

Daanen, R., Misra, D., and Thompson, A.: Frozen Soil Hydrology. Encyclopedia of Snow, Ice and Glaciers, edited by: Singh, V., Singh, P., and Haritashya, U., Springer Netherlands, 306–11, ISBN:978-90-481-2641-5, 2011.

Demontoux, F., Razafindratsima, S., Bircher, S., Ruffié, G., Bonnaudin, F., Jonard, F., Wigneron, J.-P., Sbartaï, M., and Kerr, Y.: Efficiency of end effect probes for in-situ permittivity measurements in the 0.5–6 GHz frequency range and their application for organic soil horizons study, Sens. Actuators, A: Physical, 254, 78–88, https://doi.org/:10.1016/j.sna.2016.12.005, 2017.

Demontoux, F., Tsague King, J., Bircher, S., Ruffie, G., Bonnaudin, F., Wigneron, J.-P., and Kerr, Y.: In-situ multi-frequency dielectric measurements to improve soil permittivity models for radiometric observations of soil in the high latitudes, Microrad 2020, Florence (Italy), Accepted.

Demontoux, F., Yaakoubi, G., Wigneron, G., Grzeskowiak, M., Sbartaï, M., Fadel, L., Ruffié, G., Bonnaudin, F., Oyhenart, L., Vignéras, V., Wigneron, J.-P., Villard, L., Le Toan, T., and Kerr, Y.: Antipodal Vivaldi antennas dedicated to in-situ broadband microwave permittivity measurements, 2019 European Microwave Conference in Central Europe (EuMCE), Prague (CzechRepublic), 62–65, https://prodinra.inra.fr/record/495910, 2019.

Derksen, C., Xu, X., Scott Dunbar, R., Colliander, A., Kim, Y., Kimball, J. S., Black, T. A., Euskirchen, E., Langlois, A., Loranty, M. M., Marsh, P., Rautiainen, K., Roy, A., Royer, A., and Stephens, J.: Retrieving landscape freeze/thaw state from Soil Moisture Active Passive (SMAP) radar and radiometer measurements, Remote Sens. Environ., 194, 48–62, http://dx.doi.org/:10.1016/j.rse.2017.03.007, 2017.

Dobson, M., Ulaby, F., Hallikainen, M., and El-Rayes, M.: Microwave dielectric behavior of wet soil - Part II: Dielectric mixing models, Geosci. Model Dev., GE-23, 35–46, https://doi.org/:10.1109/TGRS.1985.289498, 1985.

Entekhabi, D., Njoku, E., O'Neill, P., Kellogg, K., Crow, W., Edelstein, W., Entin, J., Goodman, S., Jackson, T., Jackson, J., Kimball, J., Piepmeier, J., Koster, R., Martin, N., McDonald, K., Moghaddam, M., Moran, S., Reichle, R., Shi, J., Spencer, M., Thurman, S., Tsang, L., and Van Zyl, J.: The Soil Moisture Active Passive (SMAP) mission, Proc. of the IEEE, 98, 704–716, http://dx.doi.org/:10.1109/JPROC.2010.2043918, 2010.

Fan, L., Wigneron, J.-P., Mialon, A., Rodriguez-Fernandez, N.J., Ai-Yaari, A., Kerr, Y., Brandt, M., and Ciais, P.: SMOS-IC Vegetation Optical Depth Index in Monitoring Aboveground Carbon Changes in the Tropical Continents During 2010–2016, IGARSS 2018 - 2018 IEEE International Geoscience and Remote Sensing Symposium, Valencia (Spain), 2825–2828, https://doi.org/:10.1109/igarss.2018.8518750, 2018.

Filali, B., Boone, F., Rhazi, J.-E., Ballivy, G.: Design and calibration of a large open-ended coaxial probe for the measurement of the dielectric properties of concrete, IEEE Trans. Microwave Theory Tech., 56, 2322–2328, https://doi.org/:10.1109/TMTT.2008.2003520, 2008.

Filali, B., Rhazi, J.-E., and Ballivy, G.: Measurement of the dielectric properties of concrete by a large coaxial probe with open end, Can. J. Phys., 84, 365–379, https://doi.org/:10.1139/p06-056, 2006.

Gower S., Vogel, J., Norman, J., Kucharik, C., Steele, S., Stow, T.: Carbon distribution and aboveground net primary production in aspen, jack pine, and black spruce stands in Saskatchewan and Manitoba, Canada, J. Geophys. Res., 102(D24), 29029–29041, https://doi.org/:10.1029/97JD02317, 1997.

Griffiths, Introduction to electrodynamics - Third Edition, Pearson, Upper Saddle River, New Jersey, 576 pp., ISBN: 978-0138053260, 1999.

Huang, J., Tsang, L., Njoku, E., Colliander, A., Liao, T., and Ding, K.: Propagation and Scattering by a Layer of Randomly Distributed Dielectric Cylinders Using Monte Carlo Simulations of 3D Maxwell Equations With Applications in Microwave Interactions With Vegetation, IEEE Access, 5, 11985-12003, doi:10.1109/ACCESS.2017.2714620, 2017.

HydraProbe Soil Sensor Manual, Revision VI, Stevens Water Monitoring Systems Inc., Portland, Oregon, United-States, 63 pp., 2018.

Jonard, F., Bircher, S., Demontoux, F., Weihermüller, L., Razafindratsima, S., Wigneron, J.-P., and Vereecken, H.: Passive L-Band Microwave Remote Sensing of Organic Soil Surface Layers: A Tower-Based Experiment, Remote Sens., 10(2), 304, https://doi.org/:10.3390/rs10020304, 2018.

Jones, S., Wraith, J., and Or, D.: Time domain reflectometry measurement principles and applications, Hydrol. Process., 16(1), 141-153, doi: 10.1002/hyp.513, 2002.

Judge, J., Galantowicz, J., England, A., and Dahl, P.: Freeze/thaw classification for prairie soils using SSM/I radiobrightnesses, IEEE Trans. Geosci. Remote Sens., 35(4), 827-832, doi:10.1109/36.602525, 1997.

Kerr, Y., Waldteufel, P., Richaume, P., Wigneron, J., Ferrazzoli, P., Mahmoodi, A., Al Bitar, A., Cabot, F., Gruhier, C., Juglea, S., Leroux, D., Mialon, A., and Delwart, S.: The SMOS soil moisture retrieval algorithm, IEEE Trans. Geosci. Remote Sens., 50, 1384–1403, https://doi.org/:10.1109/TGRS.2012.2184548, 2012.

Kerr, Y. H., Waldteufel, P., Wigneron, J. P., Delwart, S., Cabot, F. O., Boutin, J., Escorihuela, M. J., Font, J., Reul, N., Gruhier, C., and Juglea, S. E.: The SMOS mission: New tool for monitoring key elements of the global water cycle, IEEE Trans. Geosci. Remote Sens., 98, 666–687, https://doi.org/:10.1109/JPROC.2010.2043032, 2010.

Kim, Y., Kimball, K., Zhang, K., and McDonald, K.: Satellite detection of increasing northern hemisphere non-frozen seasons from 1979 to 2008: implications for regional vegetation growth, Remote Sens. Environ., 121, 472-487, http://dx.doi.org/:10.1016/j.rse.2012.02.014, 2012.

Klingshirn, C. F.: Semiconductor Optics – Graduate Texts in Physics (Chapter: Kramers–Kronig Relations), Springer, Berlin, Heidelberg, 849 pp., doi: 10.1007/b138175, 2012.

Lemmetyinen, J., Schwank, M., Rautiainen, K., Kontu, A., Parkkinen, T., Mätzler, C., Wiesmann, A., Wegmüller, U., Derksen, C., Toose, P., Roy, A., and Pulliainen, J.: Snow density and ground permittivity retrieved from L-band radiometry: Application to experimental data, Remote Sens. Environ., 180, 377-391, https://doi.org/:10.1016/j.rse.2016.02.002, 2016.

Le Vine, D. M., Lagerloef, G. S., and Torrusio, S.: Aquarius and remote sensing of sea surface salinity from space, Proc. IEEE, 98, 688–703, https://doi.org/:10.1109/JPROC.2010.2040550, 2010.

Mialon, A., Richaume, P., Leroux, D., Bircher, S., Bitar, A.A., Pellarin, T., Wigneron, J., and Kerr, Y.: Comparison of Dobson and Mironov Dielectric Models in the SMOS Soil Moisture Retrieval Algorithm, IEEE Trans. Geosci. Remote Sens., 53(6), 3084–3094, https://doi.org/:10.1109/TGRS.2014.2368585, 2015.

Mätzler, C.: Applications of the interaction of microwaves with the natural snow cover, Remote Sens. Rev., 2, 259–387, https://doi.org/:10.1080/02757258709532086, 1987.

Mavrovic, A., Madore, J.-B., Langlois, A., Royer, A., and Roy, A.: Snow liquid water content measurement using an open-ended coaxial probe (OECP), Cold Reg. Sci. Technol., 171, 102958, https://doi.org/:10.1016/j.coldregions.2019.102958, 2020.

Mavrovic, A., Roy, A., Royer, A., Filali, B., Boone, F., Pappas, C., Sonnentag, O.: Dielectric characterization of vegetation at L band using an open-ended coaxial probe, Geosci. Instrum. Methods Data Syst., 7, 195–208, https://doi.org/:10.5194/gi-7-195-2018, 2018.

Melton, J., Arora, V., Wisernig-Cojoc, E., Seiler, C., Fortier, M., Chan, E., and Teckentrup, L.: CLASSIC v1.0: the open-source community successor to the Canadian Land Surface Scheme (CLASS) and the Canadian Terrestrial Ecosystem Model (CTEM) – Part 1: Model framework and site-level performance, Geosci. Model Dev., https://13(6), 2825–2850, doi.org/:10.5194/gmd-2019-329, in review13-2825-2020, 2020.

Mériaux, S.: Contribution à l'étude de l'analyse granulométrique, Thèses présentées à la faculté des sciences de l'université de Paris, Institut national de recherche agronomique, Paris (France), Série A, 590(614), 117 pp., 1953.

Mériaux, S.: Contribution à l'étude de l'analyse granulométrique, Ann. Agron., 5(I) 5–53 and 5(II) 149–205, 1954.

Mialon, A., Richaume, P., Leroux, D., Bircher, S., Bitar, A., Pellarin, T., Wigneron, J.-P., and Kerr, Y.: Comparison of Dobson and Mironov Dielectric Models in the SMOS Soil Moisture Retrieval Algorithm, IEEE Trans. Geosci. Remote Sens., 53(6), 3084–3094, https://doi.org/:10.1109/TGRS.2014.2368585, 2015.

Mironov, V., De Roo, R., and Savin, I.: Temperature-Dependable Microwave Dielectric Model for an Arctic Soil, IEEE Trans. Geosci. Remote Sens., 48(6), 585–589, https://doi.org/:10.1109/TGRS.2010.2040034, 2010.

Mironov, V., Kosolapova, L., and Fomin, S.: Physically and Mineralogically Based Spectroscopic Dielectric Model for Moist Soils, IEEE Trans. Geosci. Remote Sens., 47(7), 2059–2070, https://doi.org/:10.1109/TGRS.2008.2011631, 2009.

Mironov, V., Kosolapova, L., Lukina, Y., Karavayskya, A., and Molostovb, I.: Temperature and texture-dependent dielectric model for frozen and thawed mineral soils at a frequency of 1.4 GHz, Remote Sens. Environ., 200, 240-249, https://doi.org/:10.1016/j.rse.2017.08.007, 2017.

Mo, T., Choudhury, B., Schmugge, T., Wang, J., and Jackson, T.: A model for microwave emission from vegetation-covered fields, J. Geophys. Res., 87, 11229–11237, https://doi.org/:10.1029/JC087iC13p11229, 1982.

Montpetit, B., Royer, A., Roy, A., and Langlois, A.: In-situ passive microwave emission model parameterization of sub-arctic frozen organic soils, Remote Sens. Environ., 205, 112-118, https://doi.org/:10.1016/j.rse.2017.10.033, 2018.

Moradizadeh, M., and Saradjian, M.: The effect of roughness in simultaneously retrieval of land surface parameters. Phys. Chem. Earth, Parts A/B/C, 94, 127–135. https://doi.org/:10.1016/j.pce.2016.03.006, 2016.

O'Kelly, B.: Accurate Determination of Moisture Content of Organic Soils Using the Oven Drying Method, Drying Technol., 22(7), 1767–1776, http://dx.doi.org/:10.1081/DRT-200025642, 2004.

Pavlov, N., and Baloshin, Y.: Electromagnetic properties of water on GHz frequencies for medicine tasks and metamaterial applications, J. Phys. Conf. Ser., 643, 012047, https://doi.org/:10.1088/1742-6596/643/1/012047, 2015.

Pardo Lara, R., Berg, A., Warland, J., and Tetlock, E.: In Situ Estimates of Freezing/Melting Point Depression in Agricultural Soils Using Permittivity and Temperature Measurements, Water Resour. Res., 56(5), e2019WR026020, https://doi.org/:10.1029/2019WR026020, 2020.

Prince, M., Roy, A., Royer, A., and Langlois, A.: Timing and spatial variability of fall soil freezing in boreal forest and its effect on SMAP L-band radiometer measurements, Remote Sens. Environ., 231, 111230, https://doi.org/:10.1016/j.rse.2019.111230, 2019.

Rautiainen, K., Parkkinen, T., Lemmetyinen, J., Schwank, M., Wiesmann, A., Ikonen, J., Derksen, C., Davydov, S., Davydova, A., Boike, J., and Langer, M.: SMOS prototype algorithm for detecting autumn soil freezing, Remote Sens. Environ., 180, 346–360, https://doi.org/:10.1016/j.rse.2016.01.012, 2016.

Rodríguez-Fernández, N. J., Mialon, A., Mermoz, S., Bouvet, A., Richaume, P., Al Bitar, A., Al-Yaari, A., Brandt, M., Kaminski, T., Le Toan, T., Kerr, Y. H., and Wigneron, J.-P.: An evaluation of SMOS L-band vegetation optical depth (L-VOD) data sets: high sensitivity of L-VOD to above-ground biomass in Africa, Biogeosciences, 15, 4627–4645, https://doi.org/:10.5194/bg-15-4627-2018, 2018.

Rowlandson, T., Berg, A., Bullock, P., Ojo, E. R., McNairn, H., Wiseman, G., and Cosh, M.: Evaluation of several calibration procedures for a portable soil moisture sensor, J. Hydrol., 498, 335–344, https://doi.org/:10.1016/j.jhydrol.2013.05.021, 2013.

Rowlandson, T., Berg, A., Roy, A., Kim, E., Pardo Lara, R., Powers, J., Lewis, K., Houser, P., McDonald, K., Toose, P., Wu, A., De Marco, E., Derksen, C., Entin, J., Colliander, A., Xu, X., and Mavrovic, A.: Capturing agricultural soil freeze/thaw state through remote sensing and ground observations: A soil freeze/thaw validation campaign, Remote Sens. Environ., 211, 59-70, https://doi.org/:10.1016/j.rse.2018.04.003, 2018.

Roy, A., Royer, A., Derksen, C., Brucker, L., Langlois, A., Mialon, A., and Kerr, Y. H.: Evaluation of Spaceborne L-Band Radiometer Measurements for Terrestrial Freeze/Thaw Retrievals in Canada, IEEE J. Sel. Top. Appl. Earth Obs. Remote Sens., 8, 4442–4459, https://doi.org/:10.1016/j.rse.2019.111542, 2015.

Roy, A., Toose, P., Williamson, M., Rowlandson, T., Derksen, C., Royer, A., Berg, A., Lemmetyinen, J., and Arnold, L.: Response of L-Band brightness temperatures to freeze/thaw and snow dynamics in a prairie

environment from ground-based radiometer measurements, Remote Sens. Environ., 191, 67-80, https://doi.org/:10.1016/j.rse.2017.01.017, 2017a.

Roy, A., Toose, P., Derksen, C., Rowlandson, T., Berg, A., Lemmetyinen, J., Royer, A., Tetlock, E., Helgason, W., and Sonnentag, O.: Spatial Variability of L-Band Brightness Temperature during Freeze/Thaw Events over a Prairie Environment, Remote Sens., 9, 894, https://doi.org/:10.3390/rs9090894, 2017b

Roy, A., Leduc-Leballeur, M., Picard, G., Royer, A., Toose, P., Derksen, C., Lemmetyinen, J., Berg, A., Rowlandson, T., and Schwank, M.: Modelling the L-band snow-covered surface emission in a winter Canadian prairie environment, Remote Sens., 10, 1451, https://doi.org/:10.3390/rs10091451, 2018.

Roy, A.R., Toose, P., Mavrovic, A., Pappas, C., Royer, A., Derksen, C., Berg, A., Rowlandson, T., El-Amine, M., Barr, A., Black, A., Langlois, A., and Sonnentag, O.: L-Band response to freeze/thaw in a boreal forest stand from ground- and tower-based radiometer observations, Remote Sens. Environ., 273, 111542, https://doi.org/:10.1016/j.rse.2019.111542, 2020.

Seyfried, M., and Murdock., M.: Measurement of Soil Water Content with a 50-MHz Soil Dielectric Sensor, Soil Sci. Soc. Am. J., 68(2), 394-403, doi:10.2136/sssaj2004.3940, 2004.

Seyfried, M., Grant, L., Du, E., and Humes, K.: Dielectric Loss and Calibration of the Hydra Probe Soil Water Sensor, Vadose Zone J., 4(4), 1070, https://doi.org/:10.2136/vzj2004.0148, 2005.

Tetlock, E., Toth, B., Berg, A., Rowlandson, T., and Ambadan, J. T.: An 11-year (2007–2017) soil moisture and precipitation dataset from the Kenaston Network in the Brightwater Creek basin, Saskatchewan, Canada, Earth Syst. Sci. Data, 11(2), 787–796, https://doi.org/:10.5194/essd-11-787-2019, 2019.

Ulaby, F., Sarabandi, K., McDonald, K., Whitt, M., and Dobson, M.: Michigan microwave canopy scattering model, Int. J. Remote Sens., 11(7), 1223–1253. doi:10.1080/01431169008955090, 1990.

Wigneron, J.-P., Jackson, T. J., O'Neill, P., Lannoy, De, de Rosnay, P., Walker, J. P., Ferrazzoli, P., Mironov, V., Bircher, S., Grant, J. P., Kurum, M., Schwank, M., Munoz-Sabater, J., Das, N., Royer, A., Al-Yaari, A., Al Bitar, A., Fernandez-Moran, R., Lawrence, H., Mialon, A., Parrens, M., Richaume, P., Delwart, S., and Kerr, Y.: Modelling the passive microwave signature from land surfaces: a review of recent results and application to the L-band SMOS and SMAP soil moisture retrieval algorithms, Remote Sens. Environ., 192, 238–262, https://doi.org/:10.1016/j.rse.2017.01.024, 2017.

Williamson, M., Rowlandson, T., Berg, A., Roy, A., Toose, P., Derksen, C., Arnold, L., and Tetlock, E.: L-band radiometry freeze/ thaw validation using air temperature and ground measurements. Remote Sens., 9(4), 403–410, https://doi.org/:10.1080/2150704X.2017.1422872, 2018.

Zhang, L., Shi, J., Zhang, Z., and Zhao, K.: The estimation of dielectric constant of frozen soil-water mixture at microwave bands. IGARSS 2003. 2003 IEEE International Geoscience and Remote Sensing Symposium. Proceedings (IEEE Cat. No.03CH37477), Toulouse (France), 4, 2903–2905, https://doi.org/:10.1109/IGARSS.2003.1294626, 2003.

Zhang, L., Zhao, T., Jiang, L., and Zhao, S.: Estimate of phase transition water content in freeze–thaw process using microwave radiometer, IEEE Trans. Geosci. Remote Sens., 48(12), 4248–4255, https://doi.org/:10.1109/TGRS.2010.2051158, 2010.

Zhao, T., Zhang, L., Jiang, L., Zhao, S., Chai, L., and Jin, R.: A new soil freeze/thaw discriminant algorithm using AMSR-E passive microwave imagery, Hydrol. Process., 25(11), 1704-1716, doi:10.1002/hyp.7930, 2011.

Zuerndorfer, B., England, A., Dobson, M., and Ulaby, F.: Mapping freeze/thaw boundaries with SMMR data, Agr. Forest Meteorol., 52(1-2), 199-225, doi:10.1016/0168-1923(90)90106-G, 1990.

Figures

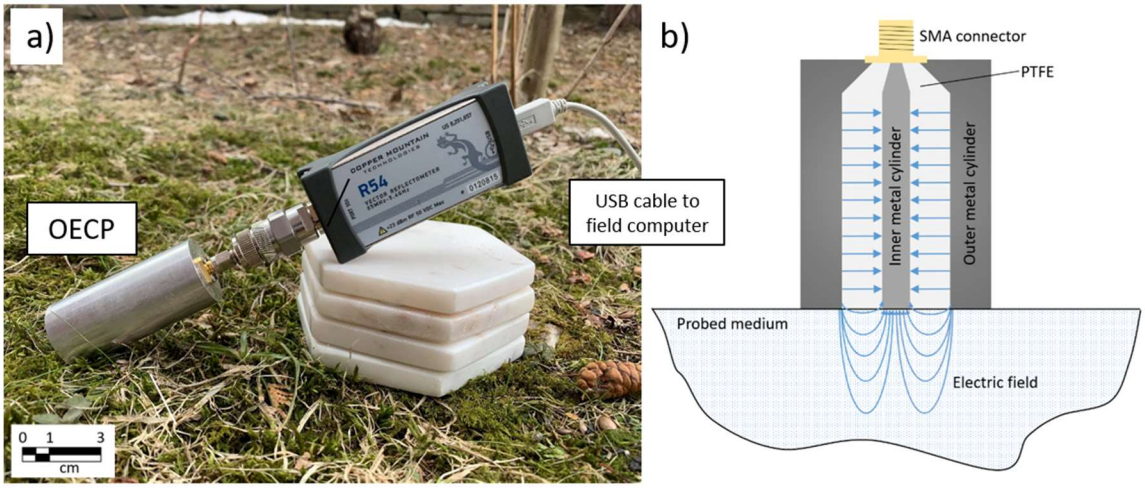

Figure 1: (a) OECP for permittivity measurement. The control program provided by the Planar R54 reflectometer manufacturer is operated with a field computer. The probe is connected to the Planar R54 reflectometer using a SMA/N cable or adaptor. (b) Diagram of the electrical field produced by the OECP.

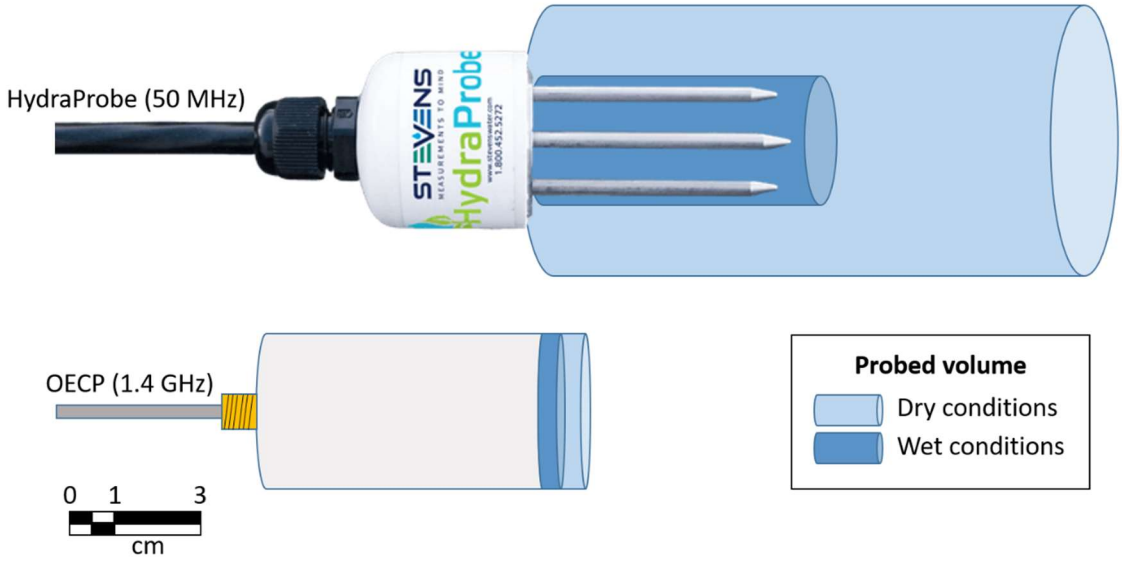

775

Figure 2: Approximate probed volume (blue) of the HydraProbe (top) and OECP (bottom) for relatively dry and wet soil conditions. The probed volume is also influenced by soil type.

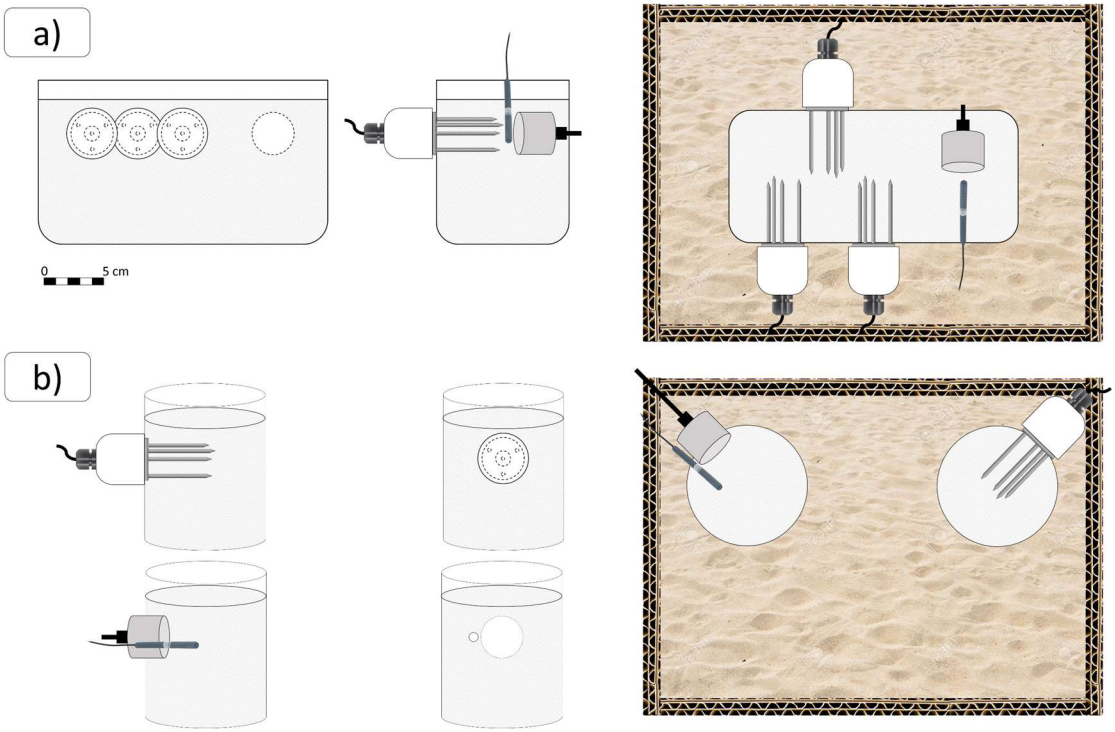

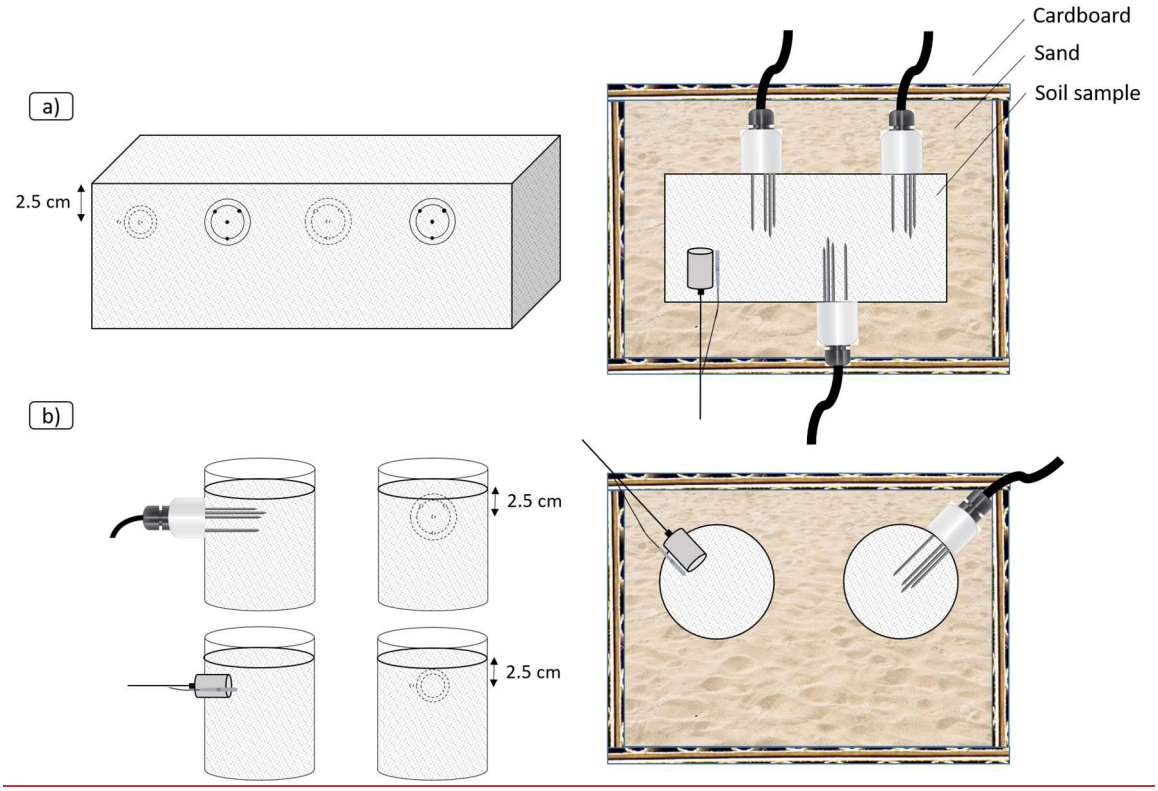

Figure 3: Top view of the cold chamber experimental setup at Guelph University (Ontario, Canada) for fast transition experiment. Setup for (a) the OBS sample, 11x24x12cm for a volume of $3.2x10^3$ cm^3 and (b) the Ontario samples, height of 12 cm and diameter of 10 cm for a volume of $9.4x10^2$ cm^3.

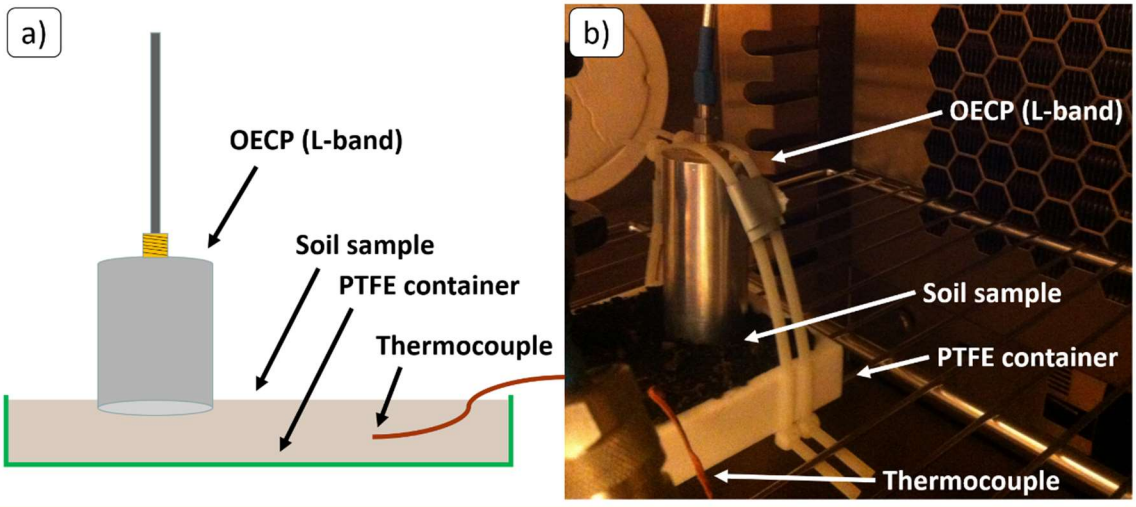

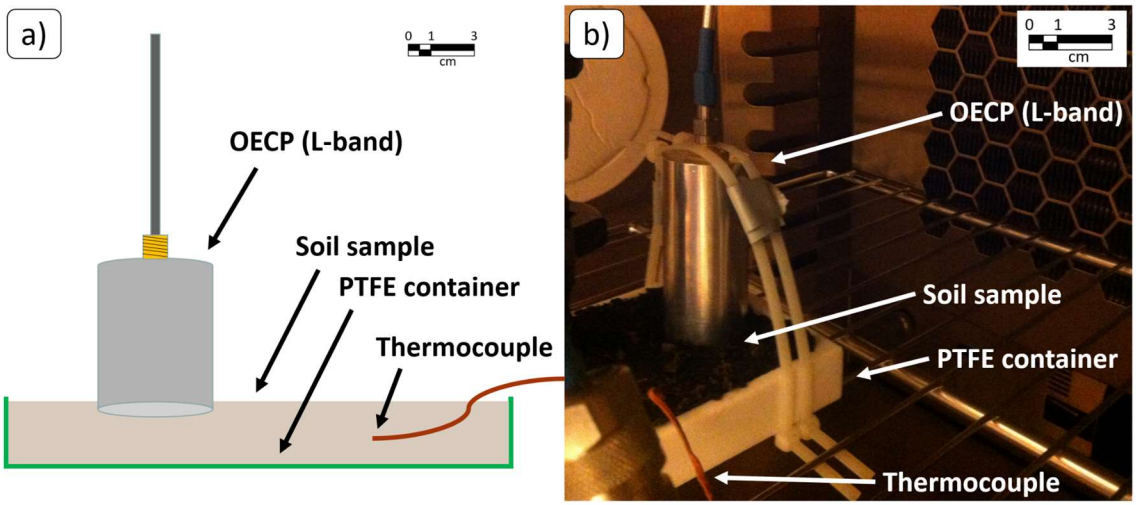

Figure 4: (a) Side view and (b) photo of the cold chamber experimental setup at the Laboratoire de l'Intégration du Matériau au Système (Bordeaux, France) for the slow freeze/thaw transition.

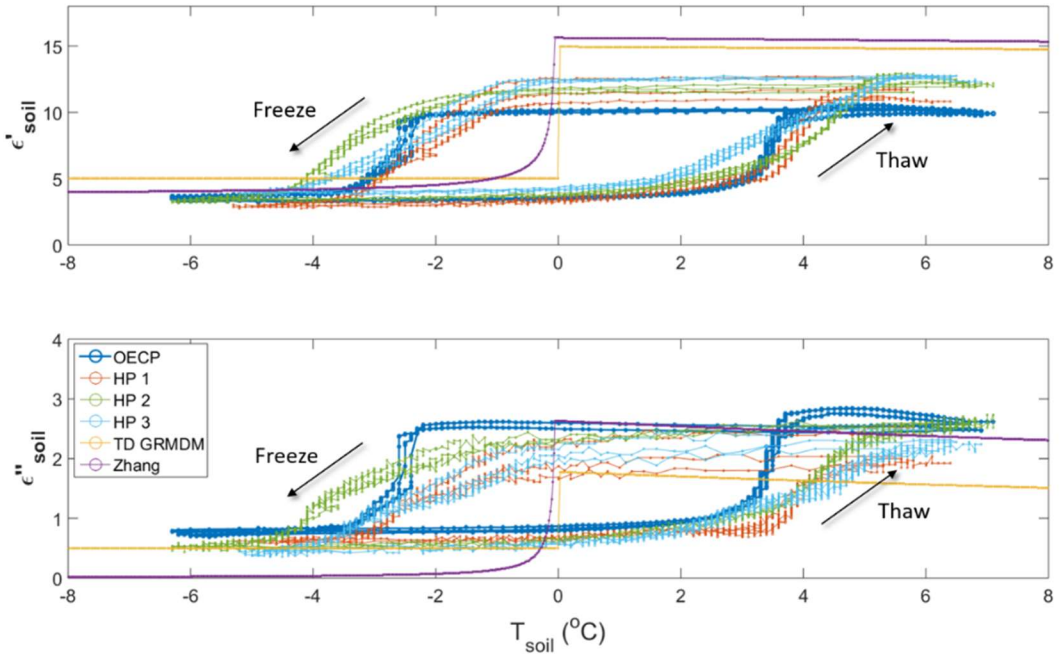

790

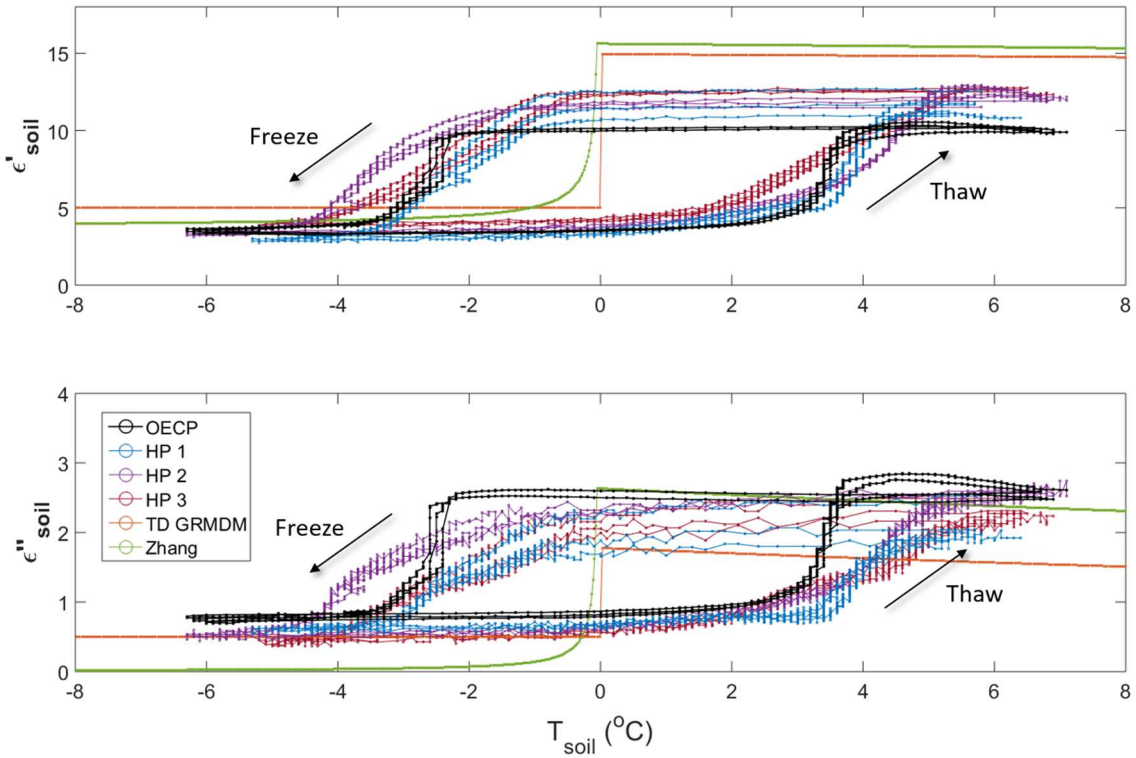

Figure 5: Real (ε') and imaginary (ε'') permittivity of an organic soil sample from the Old Black Spruce site (see Table 1) during freeze/thaw cycles in a cold chamber environment. The OECP and HP instruments monitored soil permittivity, where TD GRMDM and Zhang are model results. The hysteresis effect displayed here is amplified by the experimental setup (discussed in the text). Experiment conducted from February 1st to February 7th, 2018.

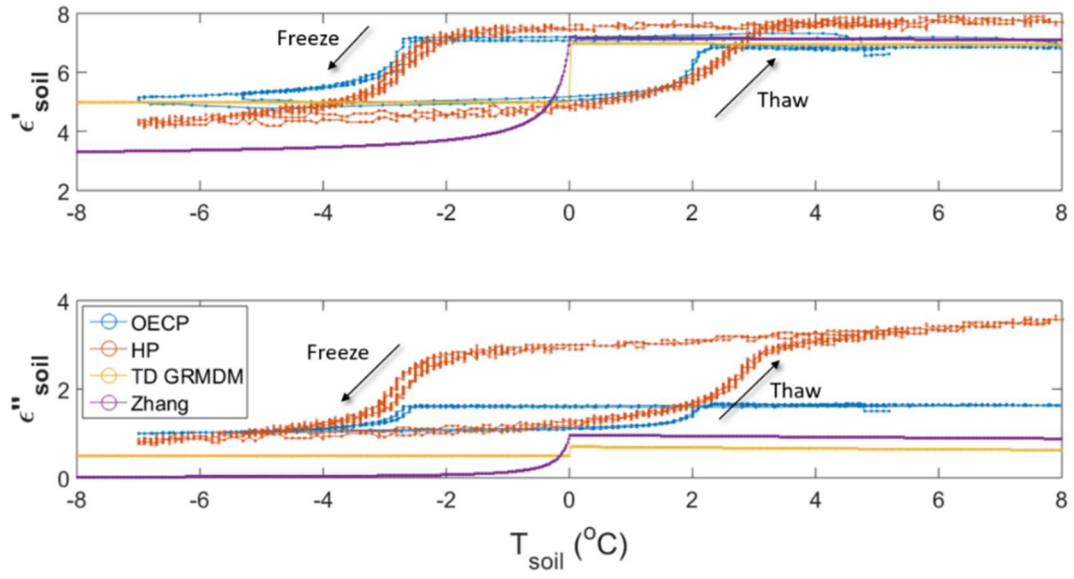

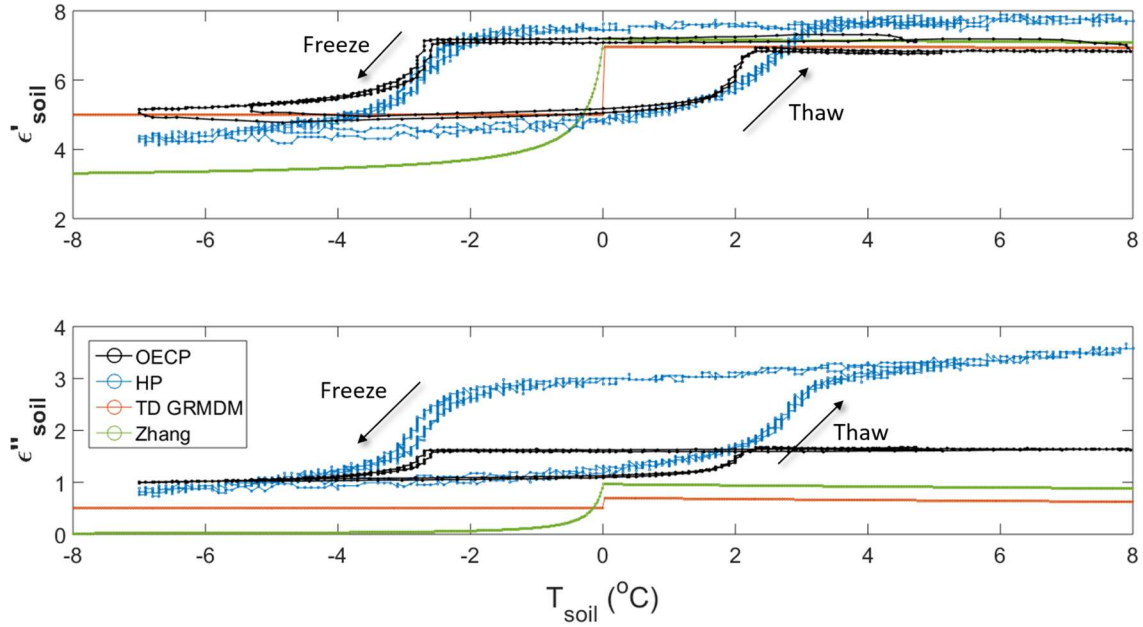

Figure 6: Same as Fig. 3 but for the sandy loam soil sample (see Table 1). Experiment conducted from April 15th to April 19th, 2018.

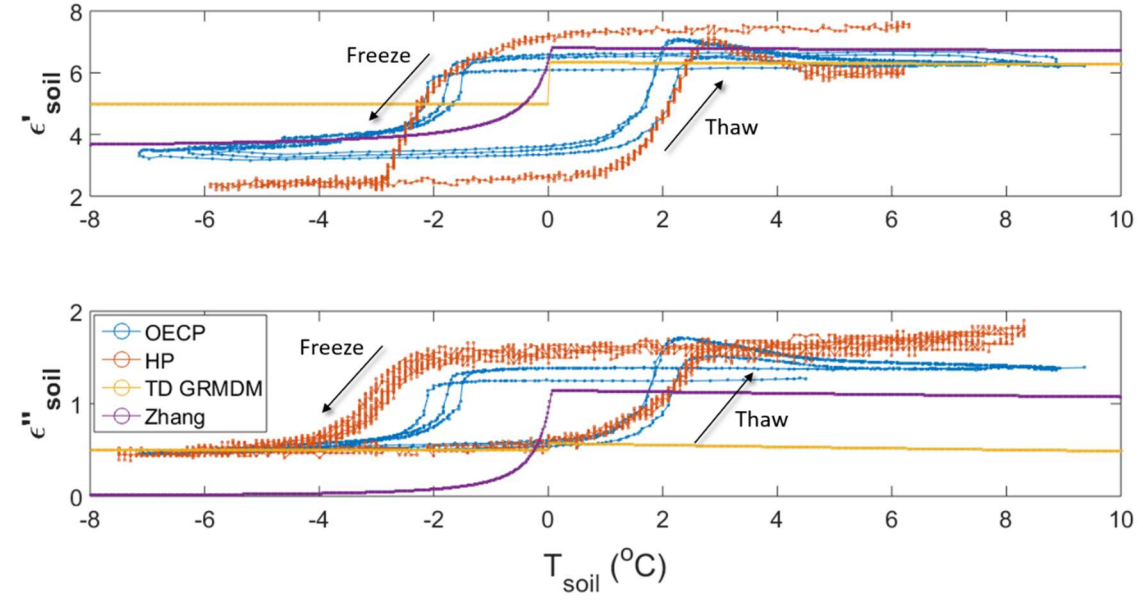

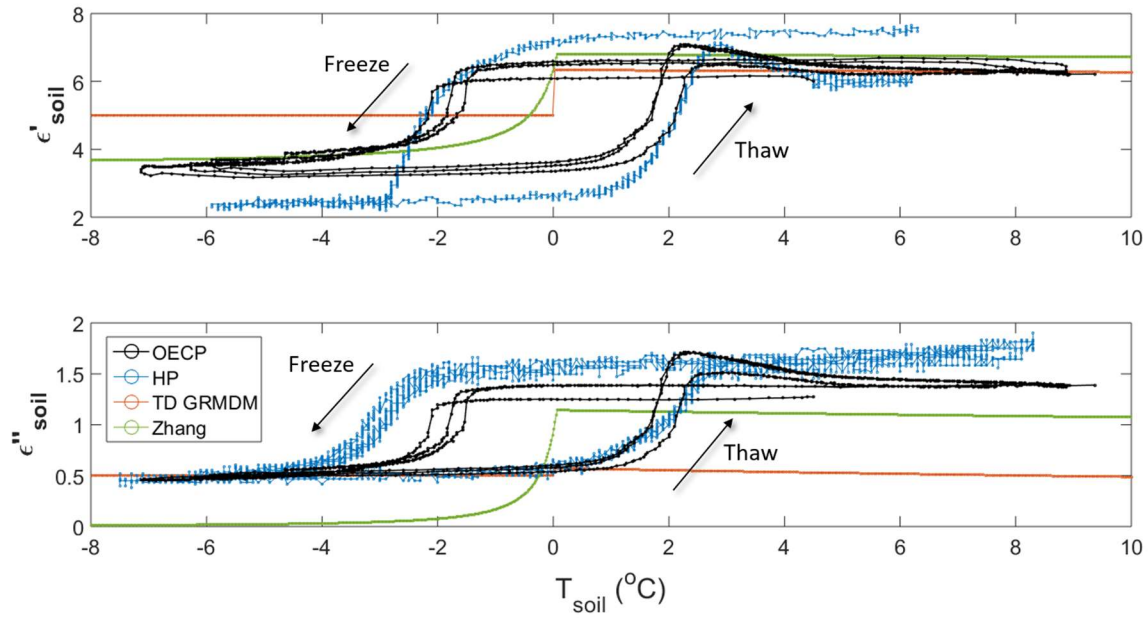

Figure 7: Same as Fig. 3 but for the loamy sand soil sample (see Table 1). Experiment conducted from March 29th to April 6th, 2018.

805

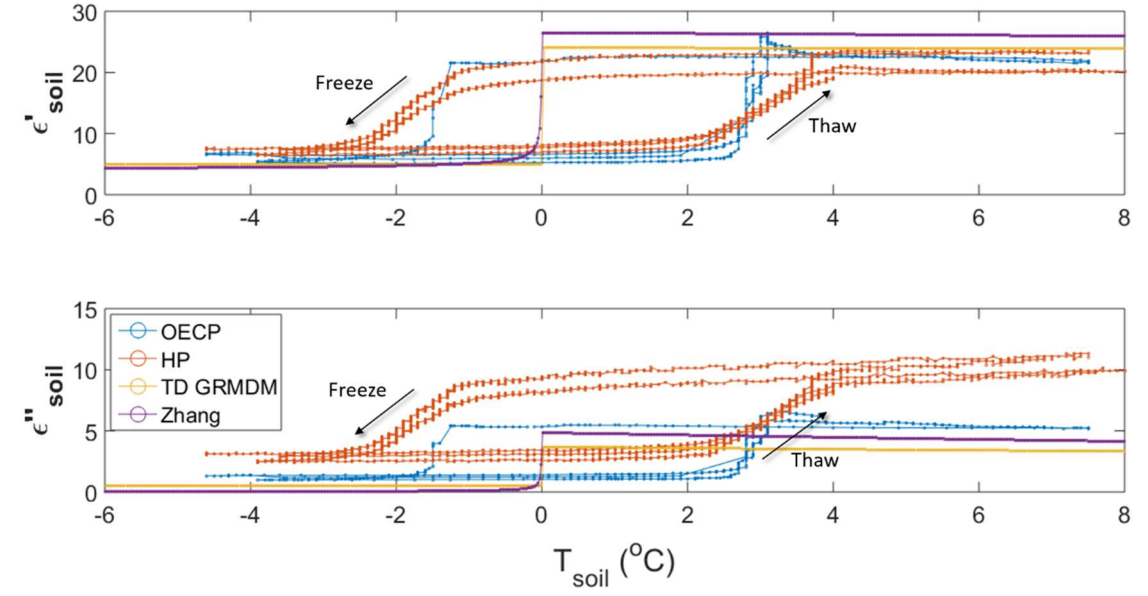

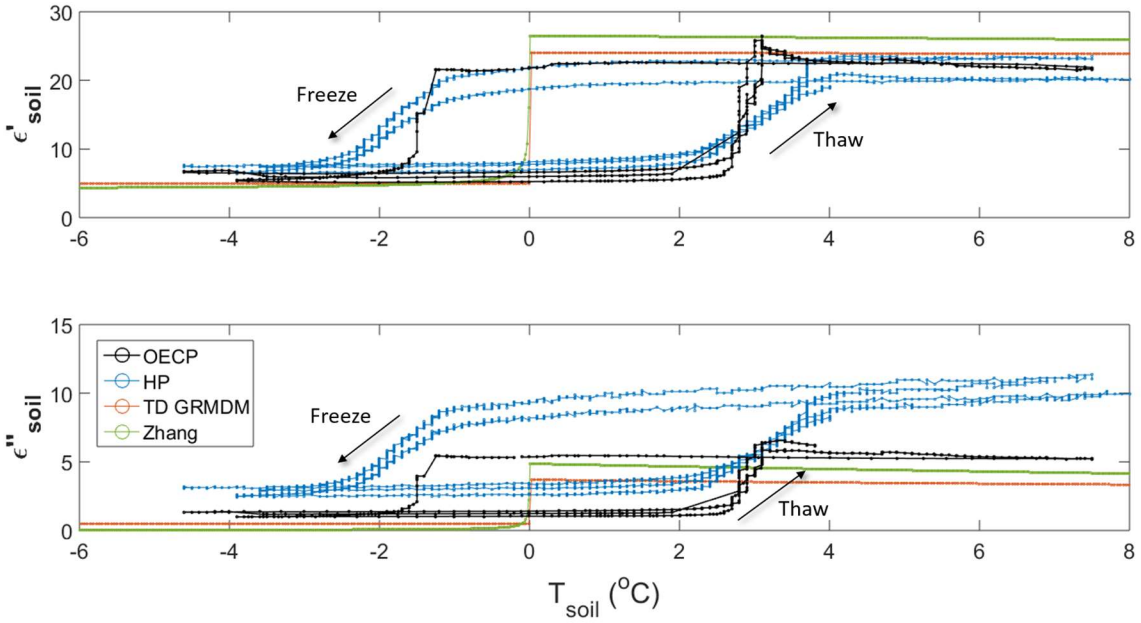

Figure 8: Same as Fig. 3 but for the clay loam soil sample (see Table 1). Experiment conducted from April 6th to April 15th, 2018.

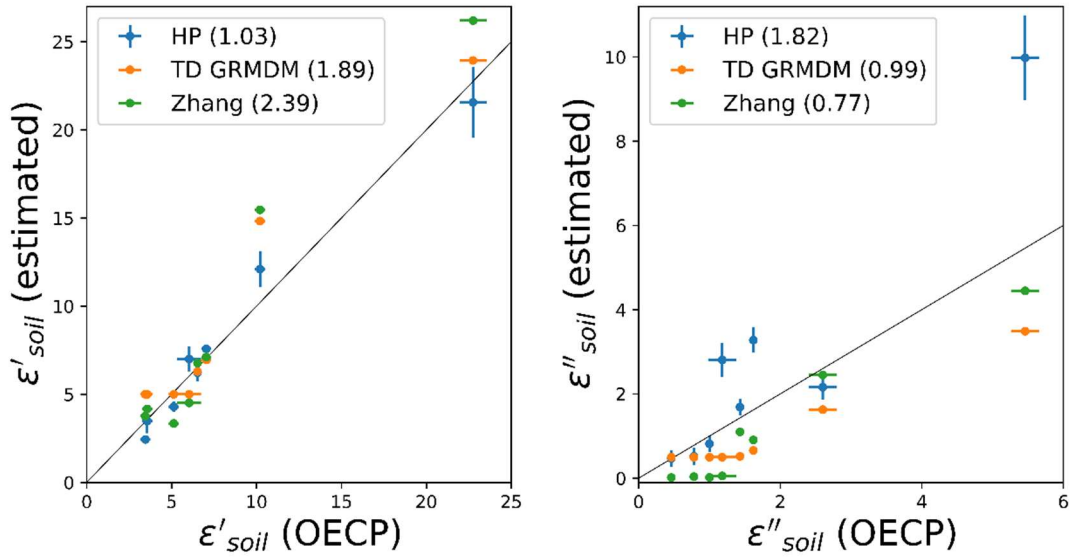

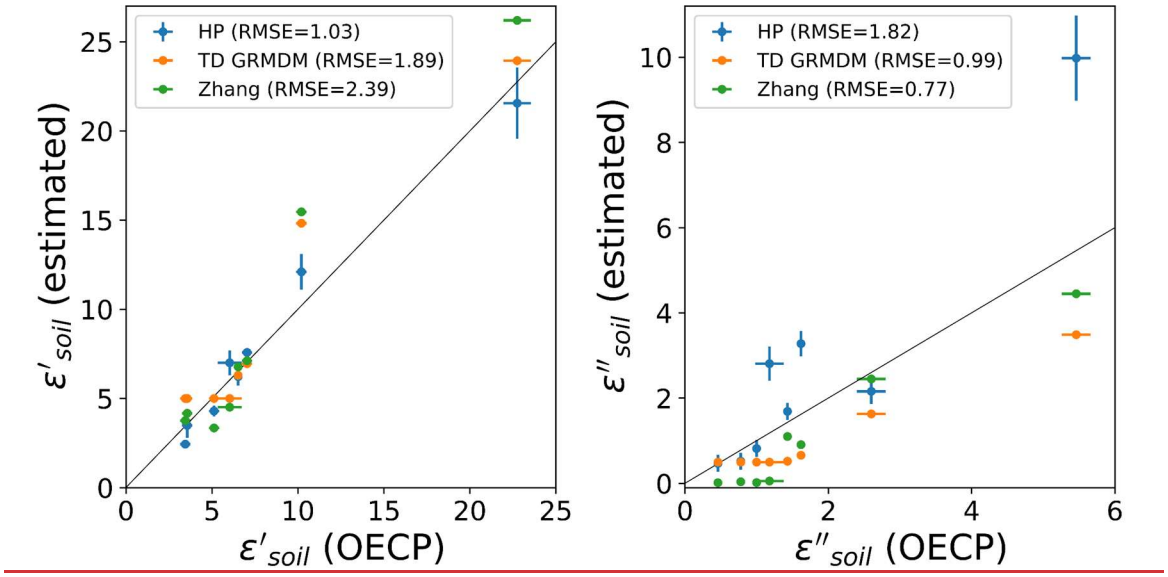

Figure 9: OECP real (ε') and imaginary (ε'') permittivity compared to HP (instrument), TD GRMDM (model) and Zhang (model) with the OECP as the reference. The black line is the 1:1 reference ratio and the root-mean square error is given in parentheses (RMSE).

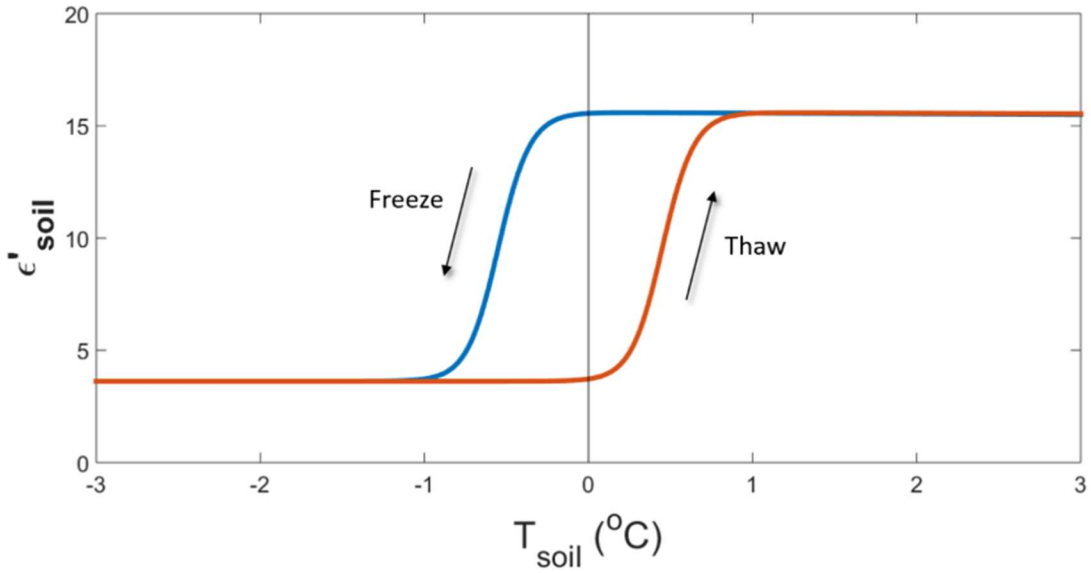

Figure 10: Expected hysteresis effect between freeze and thaw cycles. This theoretical curve was produced using an adapted version of Zhang's model and the soil composition of the OBS sample.

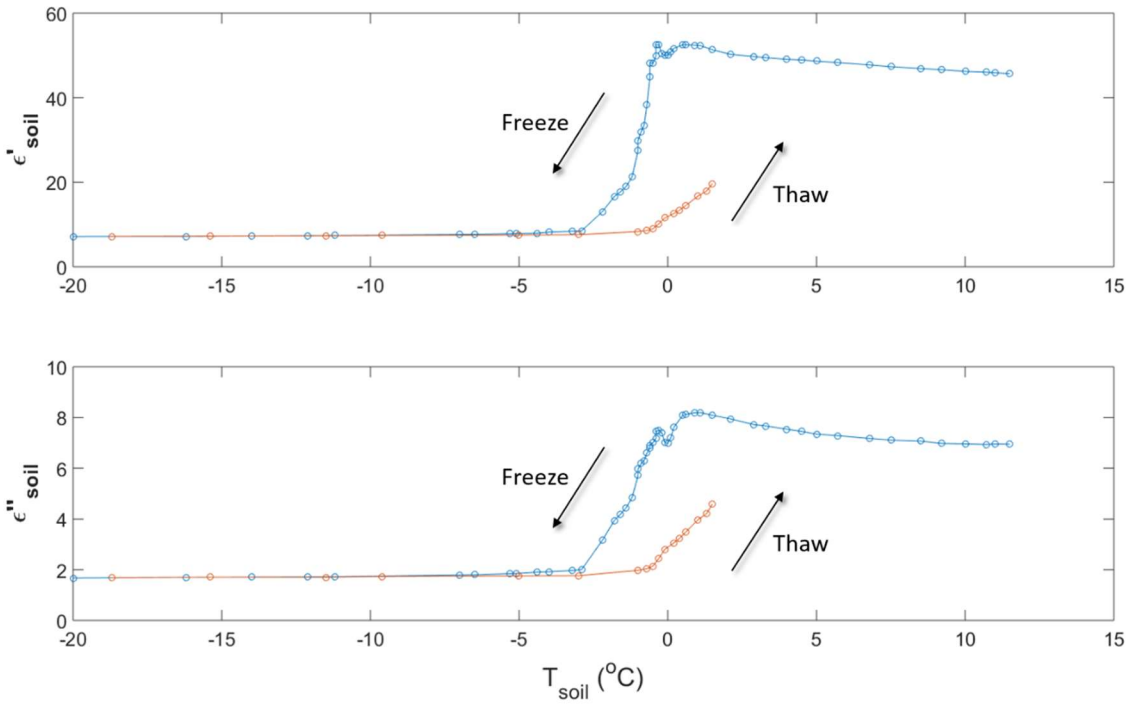

Figure 11: ~~**(a)**~~ **Real (ε') and imaginary (ε'') permittivity of an organic soil sample from the Old Black Spruce site (collected May 3rd, 2017) during a slow freeze/thaw cycle in a** ~~**cold chamber environment. (b) The OECP placed on top of an OBS soil sample to monitor soil permittivity in the Laboratoire de l'Intégration du Matériau au Système (Bordeaux, France).**~~**temperature-controlled chamber environment. Experiment conducted July 12th, 2017.**

Tables

Table 1: Soil composition and physical properties. The Old Black Spruce site is located in the boreal forest in Saskatchewan, Canada, and the three other sites are located in agricultural fields in southern Ontario, Canada. θ_V and θ_G stands for volumetric and gravimetric liquid water content, respectively. ρ_d stands for dry bulk density.

			Gravimetric composition				Physical properties		
Soil type	Site	Lattitude/ Longitude	Organic	Clay	Sand	Silt	θ_V	θ_G	ρ_d
			%	%	%	%	m^3/m^3	kg/kg	kg/m^3
Organic	Old Black Spruce	53°59′ N 105°07′ W	59	2.36	29.85	8.79	0.30	0.83	356.2
Sandy Loam	Elora	43°39′ N 80°25′ W	N/A	10	54	36	0.115	0.079	1450
Loamy Sand	Cambridge	46°26′ N 80°20′ W	N/A	2.5	78.4	19.1	0.068	0.038	1780
Clay Loam	Dunville	42°52′ N 79°44′ W	N/A	28	33	39	0.42	0.30	1400

			Gravimetric composition				Physical properties		
Soil type	Site	Lattitude/ Longitude	Organic	Clay	Sand	Silt	θ_V	θ_G	ρ_d
			%	%	%	%	m^3/m^3	kg/kg	kg/m^3
Organic	Old Black Spruce	53°59′ N 105°07′ W	59	2.36	29.85	8.79	0.30	0.83	356.2
Sandy Loam	Elora	43°39′ N 80°25′ W	N/A	10	54	36	0.115	0.079	1450
Loamy Sand	Cambridge	46°26′ N 80°20′ W	N/A	2.5	78.4	19.1	0.068	0.038	1780
Clay Loam	Dunville	42°52′ N 79°44′ W	N/A	28	33	39	0.42	0.30	1400

Table 2: Modelled and measured complex permittivity of thawed soils. The permittivity in the 5°C to 6°C temperature range (stable plateau) is averaged over the multiple freeze/thaw cycles depicted in Figs. 5 through 8. ~~Uncertainties~~Absolute and relative uncertainties (in parentheses) are based on instrument precision and measurement variability.

Soil type	$\varepsilon'_{thawed\ soil}$				$\varepsilon''_{thawed\ soil}$			
	OECP	HP	TD GRMDM	Zhang	OECP	HP	TD GRMDM	Zhang
Organic	10.2 (±0.3)	12.1 (±1.0)	14.83	15.46	2.6 (±0.2)	2.2 (±0.3)	1.63	2.45
Sandy Loam	7.0 (±0.3)	7.6 (±0.2)	6.95	7.12	1.62 (±0.04)	3.3 (±0.3)	0.66	0.91
Loamy Sand	6.5 (±0.2)	6.2 (±0.5)	6.30	6.77	1.43 (±0.05)	1.7 (±0.2)	0.52	1.10
Clay Loam	22.8 (±0.8)	21.7 (±2.0)	23.94	26.20	5.7 (±0.2)	10.0 (±1.0)	3.49	4.45

Soil type	$\varepsilon'_{thawed\ soil}$				$\varepsilon''_{thawed\ soil}$			
	OECP	HP	TD GRMDM	Zhang	OECP	HP	TD GRMDM	Zhang
Organic	10.2 (±0.3/2.9%)	12.1 (±1.0/8.3%)	14.83	15.46	2.6 (±0.2/7.7%)	2.2 (±0.3/13.6%)	1.63	2.45
Sandy Loam	7.0 (±0.3/4.3%)	7.6 (±0.2/2.6%)	6.95	7.12	1.62 (±0.04/2.5%)	3.3 (±0.3/9.1%)	0.66	0.91
Loamy Sand	6.5 (±0.2/3.1%)	6.2 (±0.5/8.1%)	6.30	6.77	1.43 (±0.05/3.5%)	1.7 (±0.2/11.8%)	0.52	1.10
Clay Loam	22.8 (±0.8/3.5%)	21.7 (±2.0/9.2%)	23.94	26.20	5.7 (±0.2/3.5%)	10.0 (±1.0/10.0%)	3.49	4.45

870

Table 3: Same as Table 2 but for frozen conditions (-5° to -6°C).

Soil type	$\varepsilon'_{frozen\ soil}$				$\varepsilon''_{frozen\ soil}$			
	OECP	HP	TD GRMDM	Zhang	OECP	HP	TD GRMDM	Zhang
Organic	3.6 (±0.3)	3.5 (±0.7)	5	4.17	0.78 (±0.04)	0.5 (±0.2)	0.5	0.039
Sandy Loam	5.1 (±0.3)	4.3 (±0.3)	5	3.35	1.00 (±0.04)	0.8 (±0.2)	0.5	0.020
Loamy Sand	3.5 (±0.3)	2.4 (±0.2)	5	3.76	0.46 (±0.04)	0.47 (±0.2)	0.5	0.017
Clay Loam	6.0 (±0.7)	7.0 (±0.7)	5	4.51	1.2 (±0.2)	2.8 (±0.4)	0.5	0.055

Soil type	$\varepsilon'_{frozen\ soil}$				$\varepsilon''_{frozen\ soil}$			
	OECP	HP	TD GRMDM	Zhang	OECP	HP	TD GRMDM	Zhang
Organic	3.6 (±0.3/8.3%)	3.5 (±0.7/20.0%)	5	4.17	0.78 (±0.04/5.1%)	0.5 (±0.2/40.0%)	0.5	0.039
Sandy Loam	5.1 (±0.3/5.9%)	4.3 (±0.3/7.0%)	5	3.35	1.00 (±0.04/4.0%)	0.8 (±0.2/25.0%)	0.5	0.020
Loamy Sand	3.5 (±0.3/8.6%)	2.4 (±0.2/8.3%)	5	3.76	0.46 (±0.04/8.7%)	0.47 (±0.2/42.6%)	0.5	0.017
Clay Loam	6.0 (±0.7/11.7%)	7.0 (±0.7/10.0%)	5	4.51	1.2 (±0.2/16.7%)	2.8 (±0.4/14.3%)	0.5	0.055

875